AD-A035 625 NEW MEXICO UNIV ALBUQUERQUE ERIC H WANG CIVIL ENGINE--ETC F/G 1/5
ANALYSIS OF AIRFIELD RUNWAY ROUGHNESS CRITERIA.(U)
NOV 76 P N SONNENBURG F29601-74-C-0030

UNCLASSIFIED FAA-RD-75-110 NL

1 OF 1
ADA035625

END

DATE
FILMED
3-77

Report No. FAA-RD-75-110

12

ANALYSIS OF AIRFIELD RUNWAY ROUGHNESS CRITERIA

Paul N. Sonnenburg

Final Report
November 1976

Prepared for

U.S. DEPARTMENT OF TRANSPORTATION
FEDERAL AVIATION ADMINISTRATION
Systems Research & Development Service
Washington, D.C. 20590

NOTICE

This document is disseminated under the sponsorship of the Department of Transportation in the interest of information exchange. The United States Government assumes no liability for its contents or use thereof.

Technical Report Documentation Page

1. Report No.	2. Government Accession No.	3. Recipient's Catalog No.
FAA-RD-75-110		

4. Title and Subtitle	5. Report Date
ANALYSIS OF AIRFIELD RUNWAY ROUGHNESS CRITERIA	November 1976
	6. Performing Organization Code
7. Author(s) Paul N. Sonnenburg	8. Performing Organization Report No. None
9. Performing Organization Name and Address Eirc H. Wang Civil Engineering Research Facility, University of New Mexico, University Hill, Campus Post Office, Albuquerque, NM 87131	10. Work Unit No. (TRAIS)
	11. Contract or Grant No. F29601-74-C-0030
12. Sponsoring Agency Name and Address U. S. Department of Transportation Federal Aviation Administration Systems Research and Development Service Washington, D.C. 20590	13. Type of Report and Period Covered Final TR 6 Nov. 1972 - 1 Feb. 1975
	14. Sponsoring Agency Code ARD-430

15. Supplementary Notes

16. Abstract

Runway roughness as it affects aircraft response and human comfort was analyzed, and two human failure criteria approaches were investigated. Although generally unsatisfactory, human-absorbed power as a criterion for roughness was found to be informative for locating severe rough areas. A third-octave band approach to establish human criteria acceleration levels was more accurate. However, this approach revealed that aircraft response data were usually far below the criteria levels for human comfort, even on runways known to be rough. Because of the lack of suitable criteria, a statistical analysis of both the roughness and the aircraft response data was performed. In this manner, profile roughness was placed on a relative basis. Statistical techniques were then described whereby both overall and detailed profile roughness properties could be classified. The establishment of detailed roughness statistics was considered incomplete, and additional work was recommended in this respect.

17. Key Words	18. Distribution Statement
Airfields Pavement Roughness Runway Profiles Roughness Criteria	Document is available to the U.S. public through the National Technical Information Service. Springfield, Virginia 22161.

19. Security Classif. (of this report)	20. Security Classif. (of this page)	21. No. of Pages	22. Price
Unclassified	Unclassified	53 45	

400 976

EXECUTIVE SUMMARY

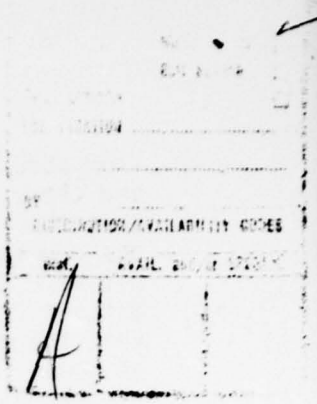

STATEMENT OF THE PROBLEM

In this work, attention is focused on runway surface roughness and its effect on aircraft vibration response which, in turn, affects passenger comfort. The basic problem is to develop the capability to state in a quantitative manner when a runway is too rough, and precisely where it is too rough. The effort is directed toward providing an airport operator with sufficient detailed information to authorize adequate repairs at a minimum cost.

RECOMMENDED PROCEDURE

The primary result of this work is the recommendation that statistical analysis of profile data be used to establish roughness criteria. This implies that aircraft vibration response data need not be considered in establishing roughness criteria, even though response data can provide supporting evidence of the degree of roughness. Hence, the aircraft itself is not a factor in the recommended approach. Statistical analysis of profile elevation data is possible if the data are filtered to remove the elevation trends which are formed by long wavelengths. A profile can then be rated according to its overall and detailed roughness properties. The standard deviation of displacement is recommended as an overall index, and the same statistic might also be considered for slopes and slope changes. The detailed roughness properties are necessary because it is likely that a profile may be generally smooth, and yet have a few severe bumps which will not be reflected in the overall index. Detailed roughness indices can be obtained by a statistical analysis of peaks (extremal analysis). The statistical approach demonstrated in this report addresses only the acquisition of the standard deviation of displacement as an overall index, and additional work is recommended. Finally, when all known indices are extracted from the profile data, each should be correlated with subjective pilot ratings, and those showing the strongest agreement should be emphasized.

APPROACHES

Indications of runway surface roughness originated from verbal complaints of pilots. For this reason, human vibration criteria were investigated first. Human response curves were found in reference 1 indicating that a peak vibration acceleration level of about 0.4 g

from about 2.0 to 20.0 Hz could be tolerated for at least 5 minutes, and there was a broad band of statistical scatter about this level. Some theoretical and experimental data revealed that a few isolated peaks reached or exceeded 0.4 g on runways claimed to be rough by pilots. However, this implied that the pilots were receiving intermittent (rather than continuous) exposure. It was therefore concluded that the material in reference 1 was insufficient, and other sources of human response data were needed.

In a second effort, an absorbed power approach was investigated. According to existing data, a human can absorb 6 W of vibration power for extended periods of time (1 minute or more). It was found that, for taxiing aircraft, the absorbed power exceeded 6 W for about 5-second intervals, once or twice during an entire run. Again, this occurred occasionally rather than continuously. Furthermore, the peak power is a function of the time interval over which the power is averaged. For example, if a 20-W peak for 1 second is averaged over 1 minute, the resulting power level is negligible. A rationale for establishing the power averaging time did not exist. It was then concluded that the absorbed power approach was more useful in locating rough regions than the 0.4 g approach, but it still could not be used to locate rough points precisely.

A final study, using human criteria, was suggested by the Aerospace Medical Research Laboratory (AMRL) at Wright-Patterson Air Force Base, Ohio. The AMRL data were in disagreement with the absorbed power results, and the 0.4 g criteria were considered obsolete. Vibration levels observed in taxiing aircraft were found to be well below comfort levels shown in the AMRL criteria, and conservative results were indicated. Evidently no additional documented information was available to pursue human response to shock, or psychologically alarming effects, at such low levels of vibration.

The influence of runway roughness on aircraft structural fatigue and avionics failure was investigated briefly. However, criteria based on these subjects, in addition to human response, relied on aircraft vibration response. The use of aircraft response as a primary tool for establishing roughness criteria was subject to question, since it was an indirect approach to the problem. It was therefore decided to pursue the more direct approach of analyzing the profiles rather than the responses.

RESULTS

A brief tabulation of the ordering of 21 available profiles according to overall displacement roughness properties is shown in table 1, where only the index of displacement standard deviation, σ, is used. Note that CVS 03 is the smoothest with σ = 0.11415 in. BGTL 16 is

seen to be the roughest with σ = 0.52756 in. By averaging the variances (the squares of the standard deviations), the average standard deviation is obtained as $\bar{\sigma}$ = 0.27882 in. Also, note that BAL 28 appears to be an average runway according to this index. However, while OKC-TE appears to be smoother than average, it contains one severe bump and is probably in need of local repair. Only a statistical analysis of peaks can determine quantitatively how rough this bump is compared to all others on all other runways.

Table 1. Profile Ordering for Displacement Roughness

Runway	σ, in.
CVS 03	0.11415
PMD 07	0.12329
DFW 17R	0.14546
IAD 01	0.15047
EDW 04	0.15947
GFK 35	0.16840
ORD 32L	0.17438
ORD 27L	0.21378
OKC TE	0.22228
CHS 15	0.26104
OKC 12	0.26589
ABQ 17	0.27368
BAL 28	0.27823
EIW 22L	0.28475
OFF 12	0.29174
ORD 22L	0.29192
JFK 13R	0.30213
BUF 05	0.36292
DCA 18	0.37457
ALB 19	0.44380
BGTL 16	0.52756

SUMMARY OF CONCLUSIONS AND RECOMMENDATIONS

Runway roughness rating methods based on aircraft response properties are not recommended. These methods consider structural, component, or human failure mechanisms, and cannot be correlated precisely with local bumps which need repair. Knowledge of aircraft response can be useful for evaluating the effectiveness of a repair plan, but its use is not justified in constructing the repair plan. The response data can also be analyzed statistically to obtain amplitude and

frequency content information for studying aircraft vibration. Collection of such data is recommended, but not as the primary information on which to base a repair plan.

The statistical analysis of filtered profile data, as demonstrated in this report, is recommended as a direct method of assessing runway profile roughness. The approach described herein is a beginning, in that only the displacement standard deviation has been extracted as a primary index of roughness. The overall properties should be expanded in the future to consider slope and slope change information. Overall properties form only half of the necessary criteria, however, and the statistical analysis of peaks is necessary before the information is complete. Finally, the correlation of the statistical information with subjective pilot ratings will complete the task.

PREFACE

This report was initially prepared by the author while at the University of New Mexico at Albuquerque, under Contract F29601-74-C-0030, Program T.D. 5.07/00. It was jointly funded by the Federal Aviation Administration and the Air Force Weapons Laboratory, Kirtland AFB, New Mexico. The author is now with the Structural Mechanics Branch, Materials System and Science Division of the U.S. Army Construction Engineering Research Laboratory (CERL), Champaign, Illinois.

Overall direction of the task was provided by Mr. L. M. Womack, Chief, Aerospace Facilities Division, Kirtland AFB. The contribution of Mr. N. E. Rinehart of the Civil Engineering Research Facility (CERF), Albuquerque, New Mexico, in performing a large portion of the computer programming and preparation of plots is acknowledged. The work of Mr. J. McCaren of CERF is also acknowledged.

COL J. E. Hays is Commander and Director of CERL and Dr. L. R. Shaffer is Technical Director. Dr. W. E. Fisher is Chief of the Structural Mechanics Branch and Dr. G. R. Williamson is Chief of the Materials and Science Division.

CONTENTS

ILLUSTRATIONS

TABLES

SECTION 1

INTRODUCTION

BACKGROUND

Runway roughness excites an aircraft's structural modes of vibration. If a part fails in an aircraft that is taxiing, it is usually because the part was substandard or the runway was too rough. In the latter case, criteria for quantitatively judging the degree of roughness of the runway are nonexistent; qualitative criteria based on individual experience are used to define the functional failure of the runway. Pavements showing structural distress are used satisfactorily until roughness or a lack of skid resistance jeopardizes the safety of the aircraft, at which time the runway is considered to have functionally failed.

In the past, numerous attempts have been made to define profile roughness independent of structural distress. At certain airfields, pilots made repeated complaints of roughness, although there was no obvious sign of pavement deterioration. It was usually not possible to precisely locate individual severe bumps, although longer and more generally rough areas could be identified. Documentation of these conditions apparently exists only in the form of informal or verbal reports. The most recent effort has been directed towards transforming such highly subjective information into quantitative human failure criteria, considering human tolerance or comfort in a shock or vibration environment.

In addition to human failure, at least two other modes of failure caused by runway roughness have been recognized but have not yet been studied to the same extent as the human mode--component failure and structural fatigue. First, maintenance of mechanical, electrical, and electronic aircraft components is expensive. Of the various environmental factors known to affect such components (e.g., vibration, temperature, humidity, sand, and dust), vibration is the most common and of major concern. Second, the degradation of the structural integrity of the aircraft is serious and catastrophic if allowed to progress. Fatigue cracks in the primary load paths of the aircraft warn of major structural failure. Unfortunately, structural fatigue is very difficult to quantify in terms of runway roughness, but from the viewpoint of safety, it is probably more important than either human or component failure.

Each of the three modes of failure mentioned above is a function of aircraft vibration response to the profile roughness. An available aircraft response computer program (the TAXI code) was used extensively

in attempts to define profile roughness criteria. Also, experimental data were collected from a Boeing 727-100 on various airfields. The interaction of the fundamental frequencies of aircraft vibration was observed in both the experimental and theoretical data, rendering the identification of individual bumps extremely difficult. For this reason, attention was focused directly on the profile data rather than the response data. Since deviations at discrete intervals along a runway are random in nature, the problem evolved into the statistical analysis of profile data.

OBJECTIVE

This research effort was undertaken to establish a quantitative approach to runway roughness as an aid to the airport operator in determining when and where repairs are needed.

SECTION 2

LITERATURE REVIEW

Information about human tolerance to vibration can be found in work by two schools of recent research activity. First, criteria based on vibration power absorbed by humans have been developed by the Mobility System Laboratory, U.S. Army Tank-Automotive Command (ATC), Warren, Michigan. Although this approach appeared to be sound, some shortcomings were discovered which rendered the technique inconclusive and not appropriate for this effort. Second, criteria based on sinusoidal and one-third octave band root-mean-square (rms) acceleration levels have been established by the Aerospace Medical Research Laboratory (AMRL), Aerospace Medical Division, Air Force Systems Command, Wright-Patterson Air Force Base, Ohio. It was thought that this approach would yield meaningful criteria, but the vibration levels obtained from actual experimental data from aircraft taxiing on runways fell substantially below the established criteria for human comfort, even in the worst cases. AMRL uses the "comfort" level as a category of human vibration exposure to distinguish it from tolerance and exposure limit environments. Some alternative criteria were provided by AMRL, but these also exceeded the levels of the real data. It became obvious that the desired criteria had to be based on a short-time or single-pulse shock phenomenon which caused alarm but was by no means strong enough to cause pain, discomfort, or loss of control of the aircraft. Therefore, a third effort was made to study psychological effects of shock and vibration on humans, but again no significant or pertinent information was uncovered in the literature search.

ABSORBED POWER APPROACH

Description

The use of absorbed power to define human tolerance to vibration is given in references 2, 3, and 4. For this method to be applicable, there must be sufficient experimental evidence that the human body can be modeled by a series of simple damped mechanical oscillators, one of which is shown in figure 1. The only mechanism which can absorb power is the damper. Physically, the damper must convert the energy it absorbs to some other form, such as heat, and dissipate this energy into the atmosphere. If some suitable ratio of power absorbed and power dissipated is not reached, the energy accumulation in the damper will cause this mechanism to become faulty or to completely fail. Therefore, if the model were applicable, the human body would exhibit signs of failure such as discomfort, pain, headache, or nausea when the absorbed power reached a certain level.

The governing equation for the vertical motion of the oscillator shown in figure 1, which can be found in numerous texts on mechanical vibration, is given as

$$\ddot{x} + 2\eta\omega_o\dot{x} + \omega_o^2 x = f(t) \qquad (1)$$

where η = damping ratio
ω_o = $\sqrt{k/m}$ = natural frequency of oscillator
k = spring constant
m = mass
x = displacement of mass
$\dot{x}$ = velocity of mass
$\ddot{x}$ = acceleration of mass
$f(t)$ = time-varying forcing function applied to mass.

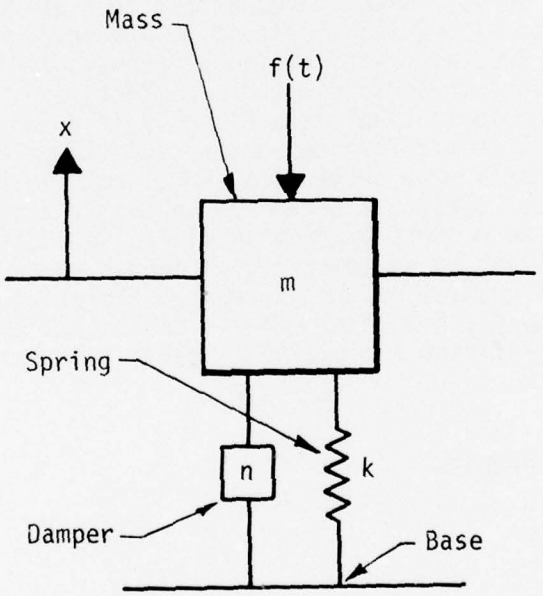

Figure 1. Simple Damped Mechanical Oscillator

The equation for calculating absorbed power is

$$P = \lim_{T\to\infty} \frac{1}{T} \int_0^T f(t)\, v(t)\, dt \qquad (2)$$

where P = absorbed power
T = time over which power is averaged
$v(t) = \dot{x}(t)$ = vibration velocity.
With an appropriate constant, P can be expressed in watts.

It is difficult to measure the forcing function, f(t), in the field; however, a transfer function technique has been developed whereby the force can be calculated if the input acceleration to the human is known. The acceleration measurement, $\ddot{x}(t)$, can be obtained with relative ease, and from it the vibration velocity can be calculated by direct integration. Furthermore, absorbed power is a scalar quantity; this implies that power generated in different directions can be added to form total power.

The constant 6-W human tolerance level is shown in figure 2 as a function of sinusoidal peak acceleration versus frequency. A vibration at a single frequency at the indicated peak g level causes 6 W to be absorbed by the human. If different discrete frequencies are present, the total absorbed power is

$$P = \frac{1}{2} \sum_{i=1}^{N} K_i A_i^2 = \sum_{i=1}^{N} K_i (A_{rms})_i^2 \qquad (3)$$

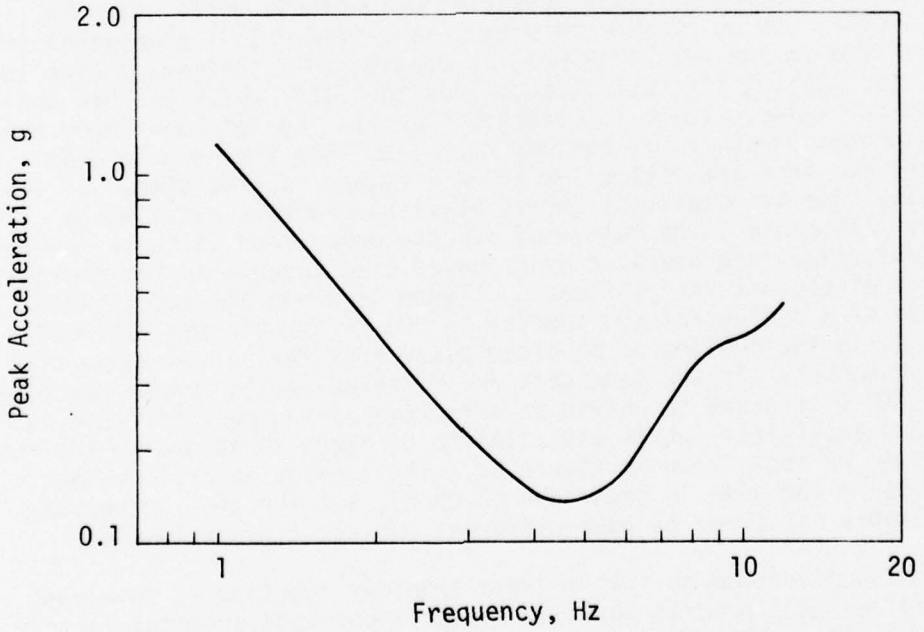

Figure 2. Constant 6-W Human Tolerance Level

where i = i^{th} discrete frequency
A_i = peak g level of i^{th} frequency
A_{rms} = rms g level
K_i = constant at i^{th} frequency
N = total number of discrete frequencies.

The absorbed power can also be calculated from a continuous spectrum of random vibration. The derivation of eq. (3), found in reference 4, shows the manipulations required in order to use the transfer function technique developed by ATC. The K_i values are the squared magnitudes of the transfer function at each discrete frequency.

Problem Areas

There were numerous reasons for rejecting the absorbed power approach for establishing human failure criteria related to aircraft vibration response from runway roughness.

First, a significant problem can be seen from eq. (2), where the power must be averaged over a finite time interval, T. If the random process is truly stationary over a sufficiently large time interval, any value of T less than total time will yield the same average power, and the selected T will not be critical. There is no established rationale for selecting the value of T, and it was demonstrated in this work (using existing aircraft acceleration response data) that the average power varies considerably as T is varied. This phenomenon is probably due to the fact that what is considered a stationary time interval for taxiing aircraft is much less than that which ATC had considered for tanks. There is evidence that ATC had not considered continuous human exposure for periods much less than 1 minute, and an aircraft can taxi the entire length of a runway in that time. If the averaging time is relatively short, occasional severe bumps while taxiing will cause large values of average power, and if these severe power excursions are averaged over longer time intervals, the overall power level becomes insignificant. Figure 3a shows the acceleration response of a Boeing 727-100 landing on DCA 36 (Washington National). Figure 3b is the continuous absorbed power plot for an averaging time of 1.28 seconds. If the same data are filtered in the manner described in the ATC literature to obtain an effective averaging time (this is not known explicitly but is estimated to be about 10 seconds), the result would be that shown in figure 3c. The average power over the total run is the same in each case (3.09 W), but the peak values are considerably different because different average times were used.

A second problem is that a human transfer function is involved; this implies that precise location of the input accelerometer is critical. In using the values of K_i furnished by ATC, the assumption (appropriate for this work) was that the acceleration measurement is taken on the seat occupied by the human (reference 4), not on the chair

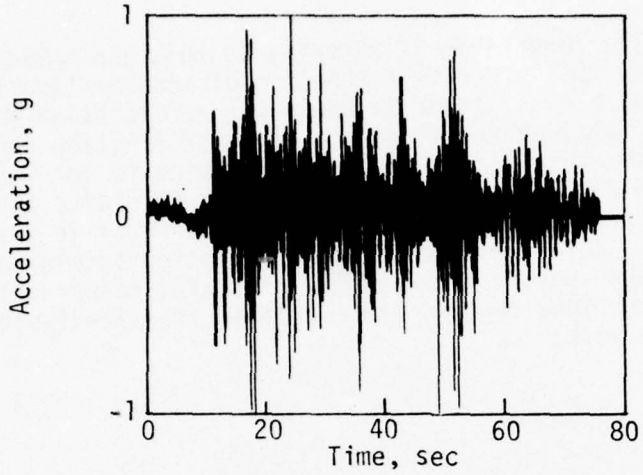

(a) Acceleration Response

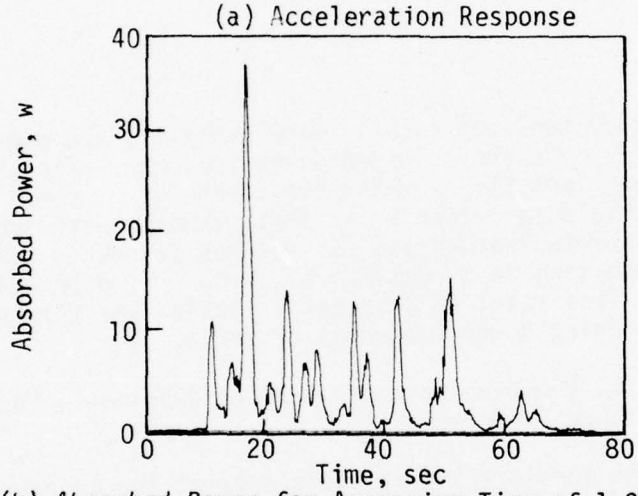

(b) Absorbed Power for Averaging Time of 1.28 Seconds

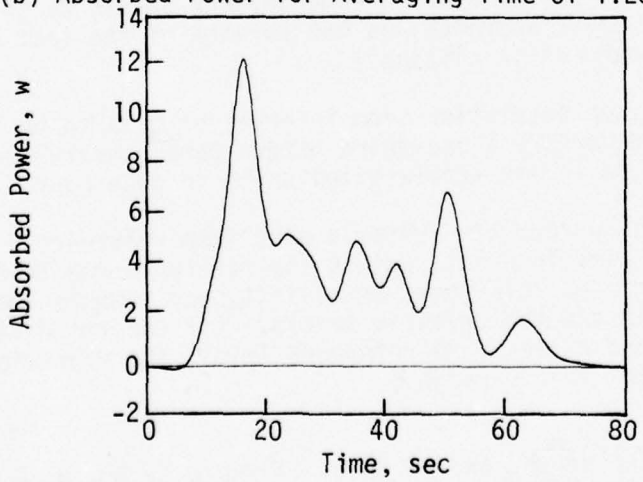

(c) Absorbed Power for Averaging Time of 10 Seconds

Figure 3. Effect of Averaging Time on Absorbed Power

frame or deck. The importance of adhering to this assumption is emphasized by noting that power is a function of acceleration squared [eq. (3)]. Hence, a small error in measuring acceleration will yield a large error in total power; also, the transfer function constants, K_i, will not be accurate if the measurement device is not located properly. To further complicate matters, reference 4* claims that changes in seat contour properties can cause large differences in transfer function values. Therefore, the fact that existing accelerometer measurements were taken on the frame of the aircraft, rather than on the top of the seat cushion, renders the available transfer function inapplicable for this work.

THIRD-OCTAVE BAND APPROACH

Description

The third-octave band approach is more generally accepted (on an international basis) than the absorbed power approach. The third-octave band approach, details of which are given in reference 5, has been empirically developed primarily at AMRL. Humans were subjected to vibration at discrete frequencies, in various frequency bands, and in broad bands, resulting in a considerable amount of data which was analyzed by AMRL. This resulted in a set of tables and charts which can be used for defining human roughness criteria.

To apply the third-octave band approach to this work, the following steps must be taken (reference 5):

(1) Obtain the acceleration response data at the appropriate input point on the human. (The correct point, as in the absorbed power approach, is the surface of the seat on which the human is sitting.)

(2) Select a representative time interval of data to be analyzed, and perform a one-third octave band spectral analysis on the data in rms acceleration units in each band.

(3) Select an appropriate criteria plot from reference 5 for the same time interval, adjust the reference rms levels for endurance, tolerance, or comfort, and compare the data rms levels and the criteria levels. (If the rms data level in any band exceeds the reference level, the vibration environment is too rough.)

*There is a critique at the end of this reference by Dr. H. E. Von Gierke of AMRL which further elaborates the problems involved in using absorbed power.

A sample problem was run to describe the third-octave band technique and to demonstrate how the results compare with the criteria in determining whether or not a particular runway needs repairs. In this theoretical case, a B-52 aircraft taxiing at 60 knots along the entire length of Thule runway 16 was used.

Figure 4a shows the time history acceleration response at the pilot station (step 1). In this example, it was assumed that the measurement was taken on the surface of the seat as required; however, the TAXI code yields the vibration data as if they were measured on the frame of the aircraft.

Step 2 was accomplished in two parts; this was done for information and convenience, rather than as a necessity. First, an acceleration spectral density of a suitable time interval of the time history trace was taken. Details for obtaining the spectral density are given in reference 6. For comparison with the AMRL criteria, a minimum time interval of 1 minute was used. However, the digitizing rate and stationary data properties dictated that a 40-second time interval would be more efficient and convenient. The endurance levels for different time intervals as provided in reference 5 are shown in figure 5. Note that the shortest time of exposure criteria provided is for 1 minute (the highest curve in the plot). Therefore, for a duration of 40 seconds, the endurance level will be greater than that shown for the 1-minute criteria. Since the 40-second interval yielded conservative results when compared to the 1-minute AMRL criteria, the shorter time interval was used. The spectral density plot over the interval from 20 to 60 seconds (figure 4a) is shown in figure 4b. The resolution bandwidth was 0.159 Hz in this case, and the first two aircraft response modes occurred at 0.9 and 1.2 Hz. The spectral density plot shows a detailed picture of the dominant frequencies in the data. With the spectral data in tabulated form in computer storage, the second part of step 2 was performed by defining the third-octave frequency bands and summing the mean square acceleration levels in each band. The square root of the summed mean square levels in a band is the rms level in that band. The third-octave acceleration levels for this example, shown in figure 4c, allows a direct comparison with the criteria levels.

The result of step 3 is also shown in figure 4c. The criteria levels were taken from reference 5, where the endurance levels are tabulated for the time interval of interest (in this case, 1 minute). The endurance levels were adjusted to *comfort* levels, appropriate for this work, by decreasing them by 10 dB; this is a factor of 3.15.

A comparison of the theoretically generated data from the TAXI code and the comfort criteria shows that the criteria were exceeded in the third-octave band centered at 3.17 Hz. This evidence should be sufficient to declare the runway rough and in need of repair.

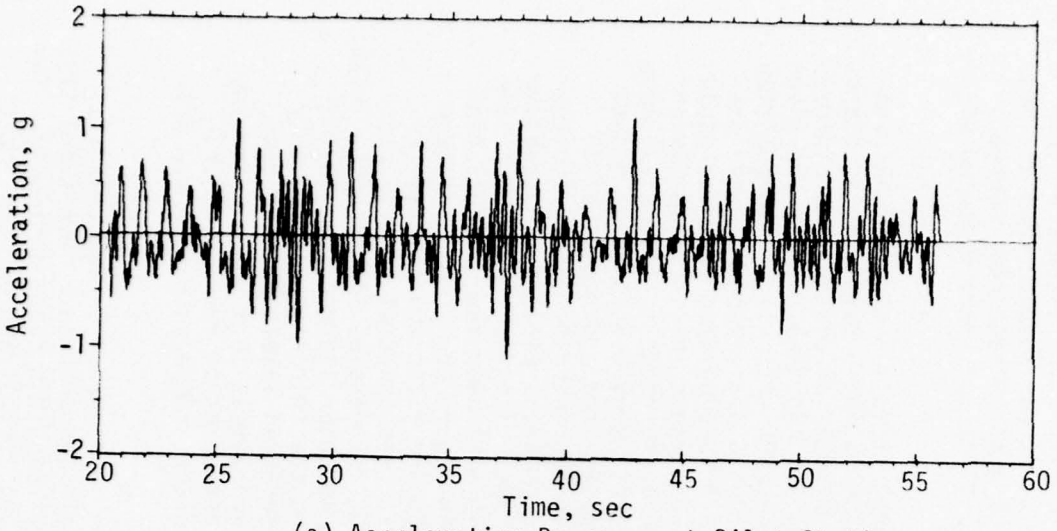

(a) Acceleration Response at Pilot Station

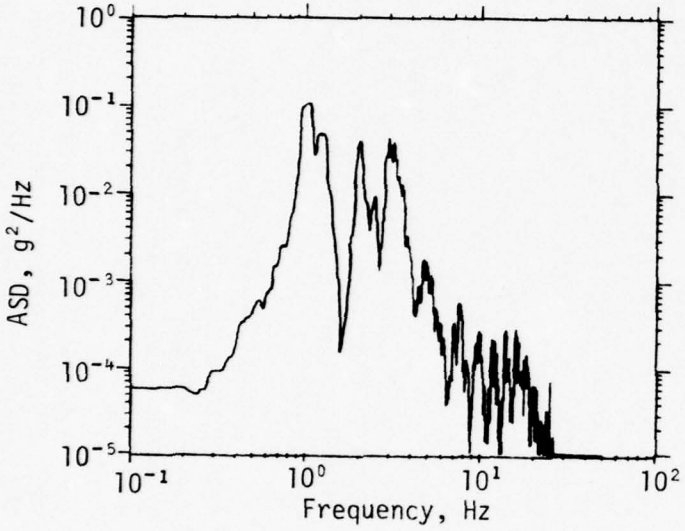

(b) Acceleration Spectral Density

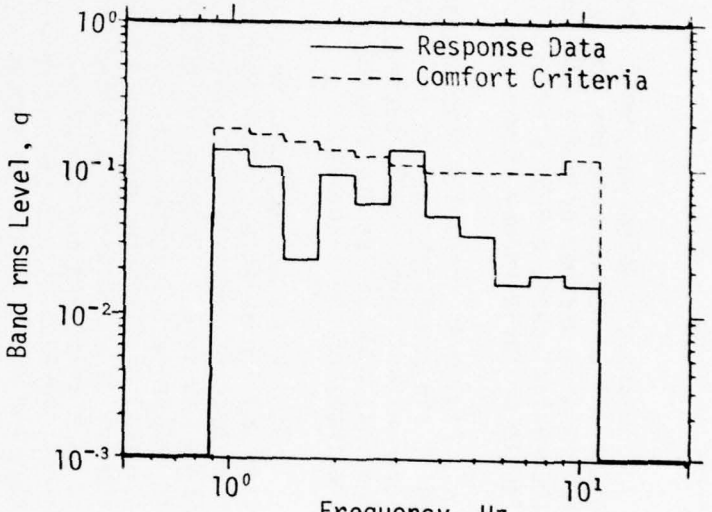

(c) Third-Octave Bands

Figure 4. Third-Octave Band Technique

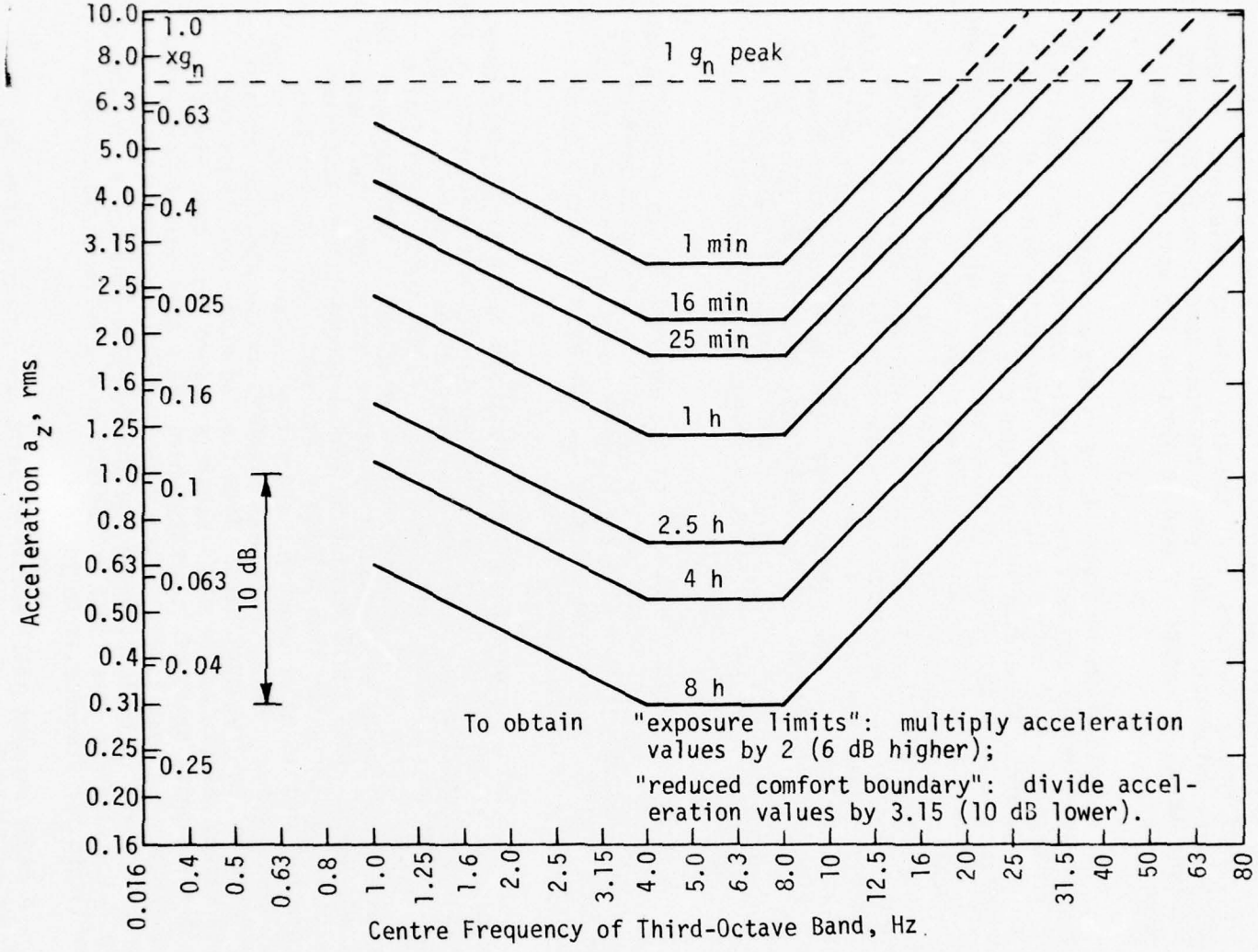

Figure 5. Third-Octave Band Criteria Levels (from reference 5)

Problem Areas

The third-octave band technique provides a quantitative overall picture of runway roughness over the time interval selected. It does not provide information about where the most severe rough spots are located; hence, it cannot be used to pinpoint the most significant rough spots.

The example shown in figure 4c is highly exceptional. Virtually all the experimental aircraft response data available were submitted to third-octave band analysis at center frequencies from 1.0 to 50.0 Hz. In general, these data fell considerably below the human comfort criteria in all bands. Figure 6 shows the result at the pilot station of a 70-knot taxi of a Boeing 727-100 on runway DAC 18 (Washington National). Although many pilots have complained about this runway, it is evident that the roughness criteria are well above the data. Furthermore, it can be demonstrated theoretically, using the TAXI code, that the response data will increase to some extent if the taxi velocity is increased. At the present time, the appropriate taxi velocity for each aircraft is not known. Therefore, in using the third-octave band approach for time intervals of about 1 minute, it is important that the appropriate taxi velocity (or range of velocities) be used for comparison with the criteria.

In view of the fact that most of the experimental data have fallen well below the comfort criteria, the question arises as to whether or not human discomfort is really the cause of pilot complaints. It may be that a pilot becomes alarmed when the landing gear hits a severe bump, and he fears structural damage.

AMRL expertise concerning other techniques which might yield more meaningful criteria was obtained. The human roughness phenonomen in this work was of shorter time duration than the smallest time interval for which ARML had collected sufficient data. It was conjectured that a time interval of 5 to 10 seconds would be meaningful, implying that the roughness phenomenon was transient in nature rather than stationary or steady-state. AMRL could furnish no formal documentation outlining pertinent criteria for time intervals less than 1 minute, but they suggested that an upper bound for short-time exposure be formed in the following manner. Allow a 1-g peak response as the absolute maximum criteria in any frequency band. Then use the equivalent sinusoidal peak values calculated for the 1-minute exposure limit from figure 5 in the frequency bands of interest, where these peak values fall below the maximum 1-g peak level. A brief tabulation of the resulting criteria is given in table 2, where the third-octave band center frequency, the calculated exposure limit criteria, and the recommended criteria are listed for frequencies up to 10 Hz.

A major problem still exists in using the criteria from the third column of table 2, in that the criteria are not approached or exceeded

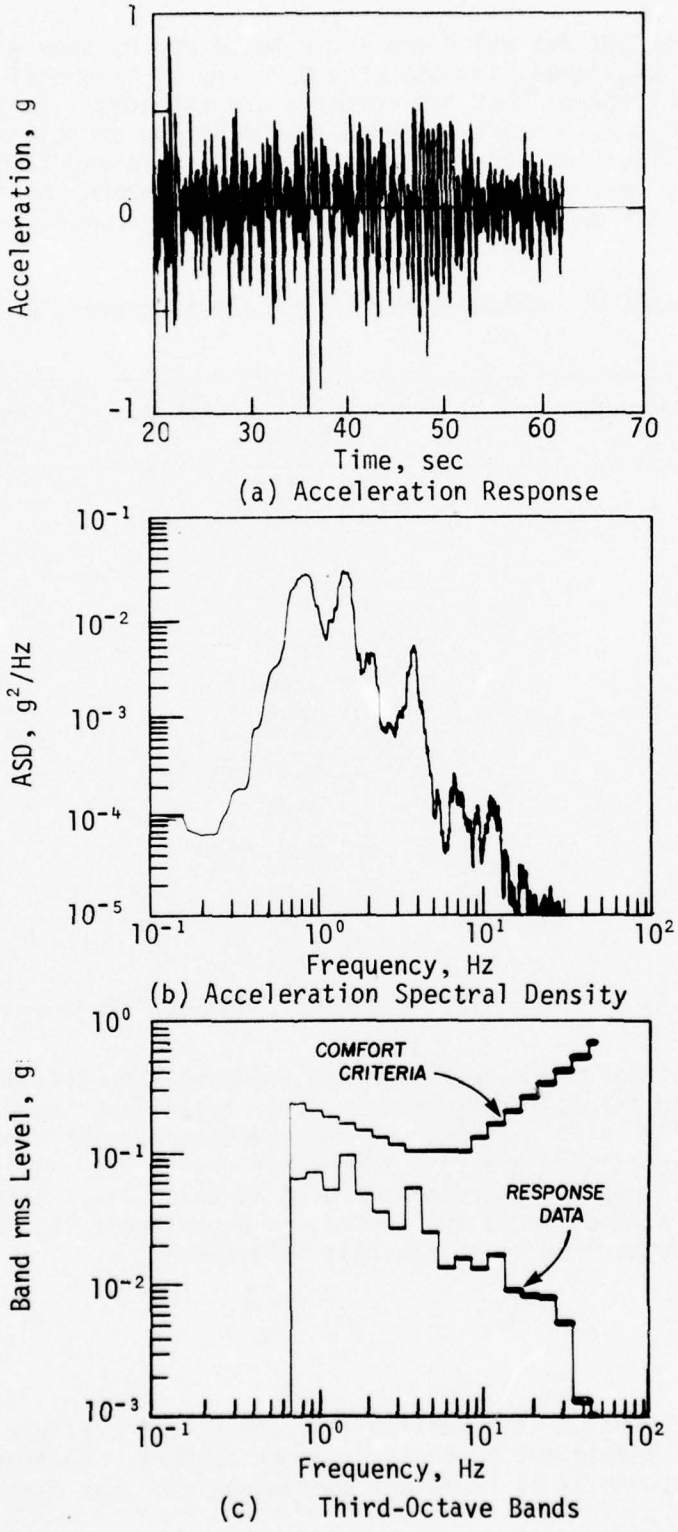

Figure 6. Typical Third-Octave Band Response Analysis

by existing profiles which are known to be rough, such as DCA 18. As previously mentioned, the use of a more appropriate taxi velocity on DCA 18 might reveal that the criteria are exceeded. It is therefore recommended that a matrix of problems be set up to determine meaningful taxi velocities for each aircraft of concern and to generate simulated responses from runways of interest to determine if the criteria in table 2 are exceeded under routine operating conditions.

Table 2. AMRL-Suggested Short-Term Exposure Criteria

Center Frequency, Hz	Exposure Limit Criteria, peak g	Allowable Criteria, peak g
1.000	1.62	1.00
1.260	1.44	1.00
1.588	1.30	1.00
2.000	1.16	1.00
2.520	1.01	1.00
3.175	0.91	0.91
4.000	0.81	0.81
5.000	0.81	0.81
6.300	0.81	0.81
8.000	0.81	0.81
10.000	1.01	1.00

The rationale for selecting the proposed AMRL criteria in table 2 has not been formally documented. Other techniques suggested by personnel at AMRL also lack adequate documentation. Therefore, although such techniques should be programmed and the results analyzed, the criteria should not be regarded as proven at this time. Either available well-documented criteria are needed, or a pertinent research effort should be authorized to obtain this information.

SUMMARY

The results of this section indicate that if failure criteria exist, they should not be based on human comfort. However, it is likely that human *alarm* is an important consideration. For example, a pilot

may taxi over a bump and become seriously concerned that the aircraft has suffered structural damage at the gear or in a major structural load path. Sufficient evidence exists from actual data that the pilot has not really suffered discomfort, even though his concern may be justified. In this event, either an aircraft structural or component failure criterion should be used, or a human alarm level should be determined and applied. A search of pertinent literature concerning human alarm as a result of shock and vibration revealed permissible levels somewhat in excess of those encountered in this work. Also, some leading studies were made to detect the possibility of firm criteria which might be derived from structural fatigue and component failure. No promising courses of action were uncovered in this respect. Attempts to establish criteria based on human, structural, or component failure always led to studying aircraft vibration response properties, and in each case the problem reduced to finding detailed rough profile spots by analyzing aircraft response data. Such approaches are, therefore, considered indirect. They reveal nothing tangible concerning criteria; they can be used to locate rough areas, but they cannot be used to locate rough spots precisely unless those spots are already obvious.

SECTION 3

STATISTICAL ANALYSIS

INTRODUCTION

Since no meaningful criteria for human alarm from short-term shocks could be found in the existing literature, a statistical approach was taken to analyze runway profiles and the corresponding aircraft response data. However, the aircraft response levels of the available data were generally much lower than the allowable human comfort levels, even for airfields pilots considered to be rough. If the statistical properties of these runways were compared to corresponding properties of other runways which are considered relatively smooth, criteria could be established. With this information recorded for all runway profiles and aircraft responses, airfields could be categorized by both overall and detailed roughness properties. The statistics for airfields known to be rough can be used as the limiting criteria.

Ample tools are available in the field of statistical analysis of random data to characterize the roughness properties of each type of data (profile and aircraft response) in a relative manner. While an absolute failure criteria cannot be established at present, very positive quantitative statements can be made that one runway is generally rougher than another, and specific rough spots can be clearly identified.

In the case of analyzing aircraft response data, no capability exists to locate rough spots precisely. However, the theoretical response data can be used to provide confidence that removal of a specific rough spot from a runway will reduce the response amplitude.

Each of the two types of random data must be analyzed differently, and each yields different meaningful information which can contribute to forming an intelligent approach to determining when and where a runway is too rough and how it should be corrected. Mathematical details for the various operations are well established in the literature; in particular, references 6, 7, and 8 were used extensively in this work.

PROFILE DATA

Analysis of profile data completely excludes reference to aircraft response properties which influence ride quality and avionics and aircraft maintenance. A direct approach using the runway profile eliminates the many variables and assumptions required when modeling aircraft

response and extending that response to an interpretation of ride quality. In addition, it is the pavement profile which must be dealt with in correcting any runway that has been defined as unacceptably rough. With this rationale, it becomes obvious that the profile should be used as a primary means to quantitatively define airfield pavement roughness.

Trend Removal

A typical runway profile (figure 7) is obtained from a list of elevations for equal increments of length (usually every 0.5 or 2.0 ft) along a runway. The overall elevation trend makes it difficult to recognize the individual bumps. Note that the elevation at the highest point of the profile is about 1000 in., while the individual bumps may not exceed 3 in.

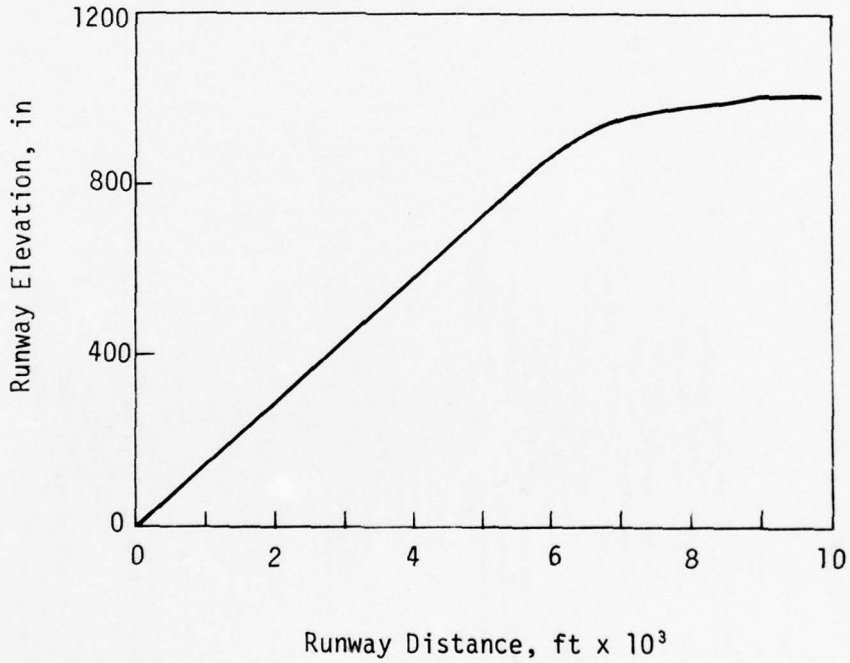

Figure 7. Raw Thule Profile (BGTL 16)

It can be demonstrated that profile wavelengths in excess of a certain limit will not significantly influence aircraft vibration response. Essentially, long wavelengths in a runway profile provide low frequency components of the aircraft forcing function. If these

frequencies are much less than the lowest mode of vibration of the aircraft, a vibration response will not be generated. Since the overall elevation trend of a profile obscures the detailed roughness properties and has no effect on aircraft response, it should be removed from the data.

In random data analysis, trend removal is a standard operation (reference 6). From the various techniques available to remove data trends, the high-pass filtering technique was chosen for this work. High-pass filtering implies that the low frequencies (wavelengths in excess of a certain limit) are removed from the data, leaving only the higher frequencies (shorter wavelengths) for subsequent analysis. Figure 8 shows the high-pass filtered data from the profile shown in figure 7. (In this case, wavelengths in excess of 400 ft were removed and the vertical scale was expanded so that the most severe rough spots could be seen clearly.) If the degree of roughness were measured only by displacement, the four roughest positive peaks would be at points A, B, C, and D. If these peaks exceeded a specific limiting displacement criterion, smoothing operations would be indicated.

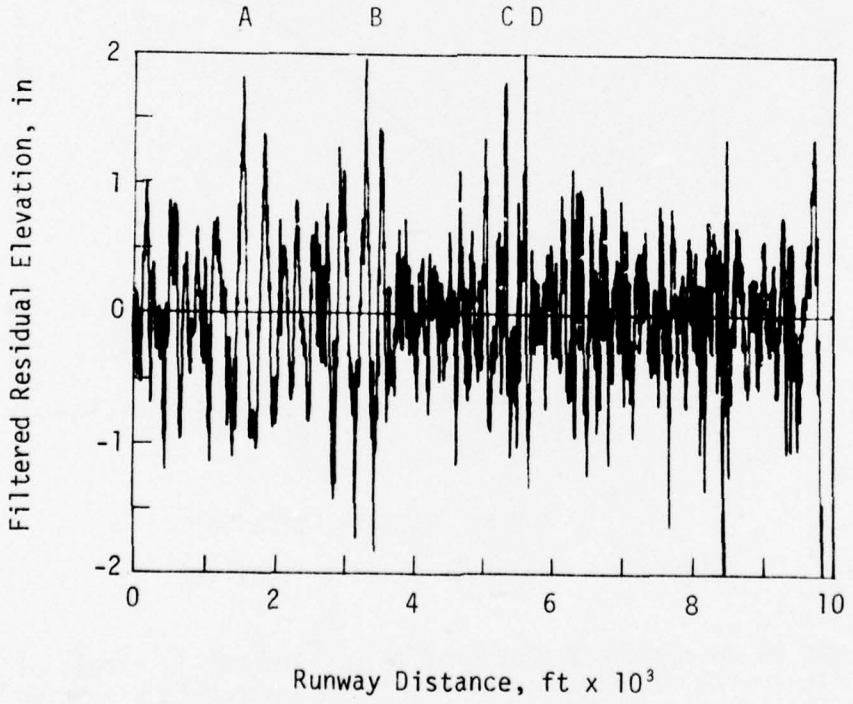

Figure 8. High-Pass Filtered Profile

The question remains as to the effect of these bumps as forcing functions on the vibration response of the various aircraft used on the runway. For example, the bump at C does not appear as rough as that at D, but it is quite possible that bump C could cause greater aircraft response. This situation could exist if Fourier transforms of short runway segments in the vicinity of the bumps revealed that bump C had the greater frequency (i.e., wavelength) content for a certain aircraft velocity, at one of the fundamental aircraft structural modes of vibration. Thus the shape of a bump can be an important factor to consider for a specific aircraft taxiing at a certain velocity. The same aircraft taxiing at a higher or lower velocity could have a lower response at C than at D as expected.

It is safe to say generally that the roughest points seen in figure 8 are the first candidates for smoothing because the bumps are truly random in nature (containing a broad band of frequencies) and aircraft response magnitude will be approximately proportional to displacement roughness. Slope and slope change roughness can also be considered once the data are filtered in this manner. However, if runway repair funds are limited, the effect of smoothing each bump individually should be studied by using the theoretical aircraft response code (TAXI) to verify that the smoothing operation will be effective for the aircraft of concern.

It is important to note that the high-pass filtered profile data (figure 8), when tabulated in digitized form, contain statistical information about roughness which can now be extracted with relative ease. The mathematics of recursive filtering are presented in references 6 and 9 and need not be discussed here. However, phase shifting must be avoided in the filtering technique selected. (See the appendix.)

Statistical Moments

The filtered profile data (figure 8) can be studied in the amplitude domain to obtain probability density and distribution functions, and the statistical moments of these functions.

Only the first four moments, denoted by μ_j, $j = 1,2,3,4$, are considered. Derivation of these moments is found in reference 8. The first moment, μ_1, is the mean value of the filtered data and is theoretically zero. Hence, the calculation of μ_1 may appear trivial. However, if μ_1 is not reasonably close to zero, the cutoff filter wavelength is too long and should be shortened. The value of μ_1 is

$$\mu_1 = \frac{1}{N} \sum_{i=1}^{N} z_i \qquad (4)$$

where z_i = the digitized points of the filtered runway data
N = the total number of points considered.

The second, third, and fourth moments are

$$\mu_j = \frac{1}{N} \sum_{i=1}^{N} (z_i - \mu_1)^j, \quad j = 2,3,4 \tag{5}$$

The most important statistic here is the second moment, μ_2, from which the overall roughness of a runway can be quantified. In the form of eq. (5), μ_2 gives the mean square value of the filtered profile. An improved second moment can be obtained by dividing by N-1 instead of N. This result is called the *unbiased variance*. However, for a large N, this improvement is trivial. The square root of μ_2 is, therefore, the rms level of the filtered profile, and this is a direct indicator of overall roughness. Since N is always large, the rms level is equivalent to the standard deviation, σ, which is the square root of the variance ($\sigma = \sqrt{\mu_2}$). The value of σ depends on the filter cutoff wavelength selected. Therefore, a suitable wavelength should be fixed for all profiles analyzed. The rationale for selecting a suitable common cutoff wavelength must be as follows:

(1) The resulting profile forcing function frequencies at appropriate aircraft velocities will not excite the aircraft's fundamental modes of vibration, and

(2) A substantial change in cutoff wavelength will not significantly change the σ value.

The cutoff wavelength is not critical, however, and a value of 400 ft was used. Therefore, rigorous satisfaction of conditions (1) and (2) has not been attempted in this work.

To define notation, it is convenient to discuss the probability density and distribution functions. This information can be found in any basic statistical text. Typical density and distribution functions are shown in figure 9. Figure 8 represents a typical filtered profile, $z(x)$, where z is the displacement amplitude and x is distance along the runway. With N the total number of digitized points in the trace and Δz a suitable increment of amplitude, the probability of the signal lying in the selected Δz increment is

$$P_i = \frac{n_i}{N\Delta z} \tag{6}$$

where n_i = the number of data points in the i^{th} increment.
For a sufficiently small Δz, p_i can be plotted as a function of z as shown in figure 9a. The density function, $p(z)$, would be bell-shaped, as shown, with certain mathematical properties if the data were

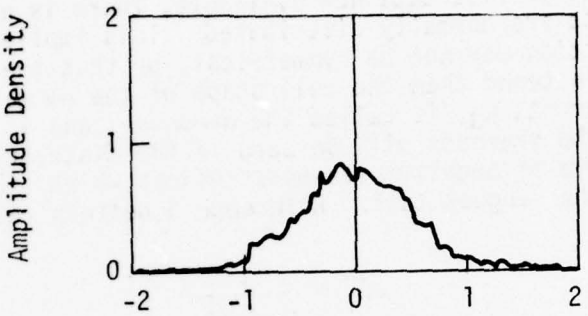

(a) Density Function

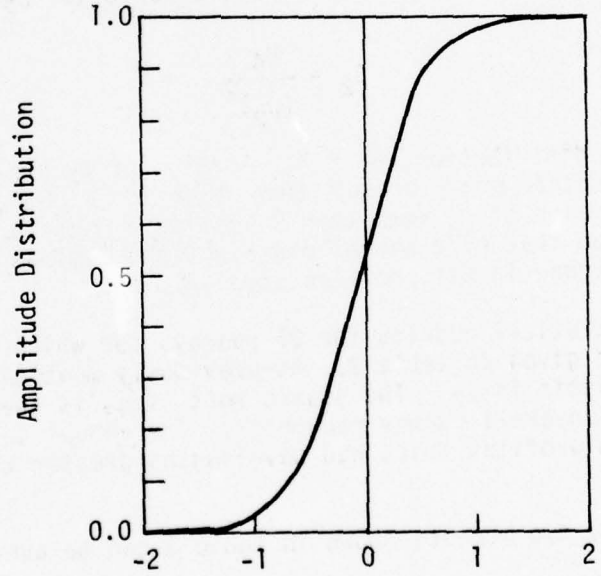

(b) Distribution Function

Figure 9. Profile Density and Distribution Functions

normally distributed. In this case the mean value, μ_1, would be zero and p(z) would taper to zero at approximately $\pm 3\sigma$ (three times the standard deviation). The area under p(z) is unity, and the probability distribution function, P(z), is the integral of p(z) as shown in figure 9b. Figure 9 thus furnishes a convenient graphical representation of the statistical properties of a filtered profile.

With the profile data now available, there is no reason to assume that the data are normally distributed. This implies that a typical density function may not be symmetrical, or that the shape may be more peaked or flattened than the bell shape of the normal distribution. The third moment, μ_3, is called the *skewness*, and it is a measure of symmetry. The skewness will be zero if the distribution is symmetrical. Positive or negative skewness defines which side of the distribution has the longest tail. Reference 8 defines relative skewness as

$$\sqrt{\beta_1} = \frac{\mu_3}{(\mu_2)^{3/2}} \tag{7}$$

An average skewness property for a collection of numerous runways might reveal a construction or settlement trend common to all runways.

The fourth moment, μ_4, is called *kurtosis* and is a measure of the flatness or peakedness of the distribution function. This property is more meaningful if expressed as relative kurtosis, β_2:

$$\beta_2 = \frac{\mu_4}{(\mu_2)^2} \tag{8}$$

For a normal distribution, $\beta_2 = 3$. A value of β_2 greater than 3 implies a density function more peaked than that of a normal distribution; likewise, a value of β_2 less than 3 implies a density function more flattened than that of a normal distribution. Values of β_2 greater than 3 were found in all profiles studied.

The statistical results for 21 runways for which profiles were available are given in table 3. As previously mentioned, the most important statistic is μ_2. The square root of μ_2 is the σ value and the best index of overall runway roughness. The values in table 3 were obtained from profiles which had wavelengths greater than 400 ft filtered out.

The first two moments shown in table 3 can be averaged:

$$\bar{\mu}_j = \frac{1}{K} \sum_{i=1}^{K} \mu_{ij} \quad \begin{matrix} i = 1,K \\ j = 1,2 \end{matrix} \tag{9}$$

where K = the total number of profiles

Table 3. Profile Statistical Results

Ident. Index	Runway	Number of Points Averaged	Mean (μ_1)	Mean Square (μ_2)	RMS (σ)	Skewness (μ_3)	Relative Skewness ($\sqrt{\beta_1}$)	Kurtosis (μ_4)	Relative Kurtosis (β_2)	Roughness Order
1	DCA 18	3337	0.00336	0.14043	0.37456	-0.00665	-0.12637	0.07122	3.6115	19
2	CHS 15	4408	-0.00153	0.06814	0.26104	0.00323	0.18159	0.03180	6.8489	10
3	GFK 35	5477	-0.00030	0.02836	0.16840	-0.00011	-0.02303	0.00383	4.7620	6
4	OFF 12	4687	0.00031	0.08511	0.29174	0.01530	-0.61620	0.05705	7.8758	15
5	CVS 03	3789	0.00034	0.01303	0.11415	-0.00008	-0.05379	0.00060	3.5340	1
6	OKC 12	3139	0.00150	0.07070	0.26589	0.00107	0.05712	0.01917	3.8340	11
7	OKC TE	3613	0.00084	0.04941	0.22228	-0.00139	-0.12682	0.01656	6.7843	9
8	ABQ 17	4309	0.00047	0.07490	0.27368	-0.00882	-0.43005	0.02917	5.1995	12
9	BGTL 16	4912	-0.00031	0.27832	0.52756	-0.02153	-0.14663	0.32915	4.2492	21
10	ORD 22L	3940	0.00056	0.08522	0.29192	-0.00441	-0.17727	0.04240	5.8383	16
11	ORD 27L	4972	0.00083	0.04570	0.21378	0.00178	0.18220	0.01182	5.6596	8
12	ORD 32L	5700	-0.00085	0.03041	0.17438	-0.00307	-0.57914	0.00574	6.2090	7
13	BUF 05	3951	0.00097	0.13171	0.36292	-0.01910	-0.39958	0.10261	5.9150	18
14	DFW 17R	5900	0.00012	0.02116	0.14546	0.00027	0.08772	0.00489	10.921	3
15	ALB 19	2904	-0.00500	0.19696	0.44380	0.04595	0.52568	0.26472	6.8239	20
16	JFK 13R	7009	-0.00146	0.09128	0.30213	-0.00395	-0.14323	0.13816	16.582	17
17	BAL 28	4620	0.00931	0.07741	0.27823	0.01133	0.52606	0.12637	21.089	13
18	IAD 01	5392	-0.00012	0.02264	0.15047	-0.00294	-0.86304	0.00342	6.6723	4
19	EWI 22L	4540	0.00020	0.08108	0.28475	0.00116	0.05024	0.02506	3.8120	14
20	EDW 04	7407	0.00002	0.02543	0.15947	-0.00020	-0.04932	0.00205	3.1700	5
21	PMO 07	4903	0.00004	0.01520	0.12329	-0.00041	-0.21879	0.00142	6.1461	2

$\overline{\mu}_j$ = the average j^{th} moment.

However, the σ values cannot be averaged in this manner; this quantity must be obtained from the average of μ_2. For the 21 available profiles, the average rms, $\overline{\sigma}$, value was calculated as

$$\overline{\sigma} = \sqrt{\overline{\mu}_2} = 0.279 \text{ in.} \qquad (10)$$

This property becomes more descriptive and meaningful as the number of profiles is increased.

The σ values in table 3 provide a direct comparison of overall roughness and may be compared to the average $\overline{\sigma}$ level. Runway BGTL 16 (Thule) was the roughest with σ = 0.528 in.; CVS 03 (Cannon) was the smoothest with σ = 0.114 in.

Usually, the 3σ level of a distribution is considered significant, in that deviations greater than 3σ comprise a large percentage of the data. For example, in a normal distribution, 99.6 percent of the data falls below the 3σ level. Using this criterion with the average standard deviation gives $3\overline{\sigma}$ = 0.837 in. The percent value is not known since the kurtosis factors being greater than 3 implies that the distributions are not normal. The raw and filtered profiles for DCA 18 (Washington National) are shown in figure 10. The $\pm 3\overline{\sigma}$ levels are shown as dotted lines in the filtered profile (figure 10b). These reference levels are exceeded several times in each direction in this profile of a runway which has been described as very rough by numerous pilots. It is important to note that the precise locations of the rough spots are available in the digitized data, and that they are graphically obvious in the profile. Furthermore, a value of σ = 0.375 in. for DCA 18 shows that it is definitely rougher generally than the average profile with $\overline{\sigma}$ = 0.279 in. This demonstrates how both the detailed and overall roughness properties of a profile are quantified. However, the location of severe peaks in this manner is considered crude, and may yield nonconservative estimates of extreme peaks. A more thorough analysis of the peaks using the statistics of extreme values is preferred.

Additional Significant Distributions

There are at least two other useful statistical distributions which can be extracted from the data. An example of overall roughness statistics is the rms (or $\overline{\sigma}$) level in table 3. Equal consideration might be given to the standard deviation of slopes and slope changes, but there was insufficient time to obtain these indices for this report. When these rms values are compared, one profile is found to be generally rougher than another in a direct manner. Since these rms values

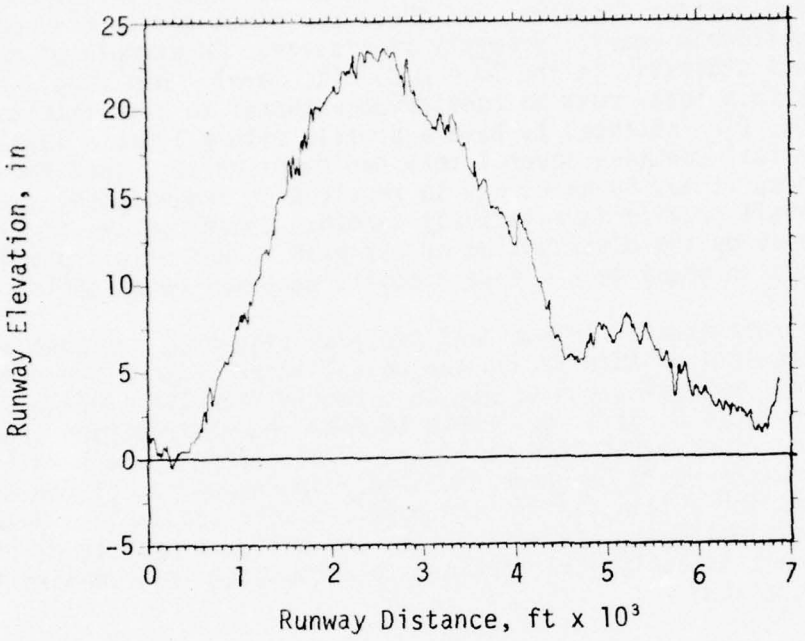

(a) Raw Profile

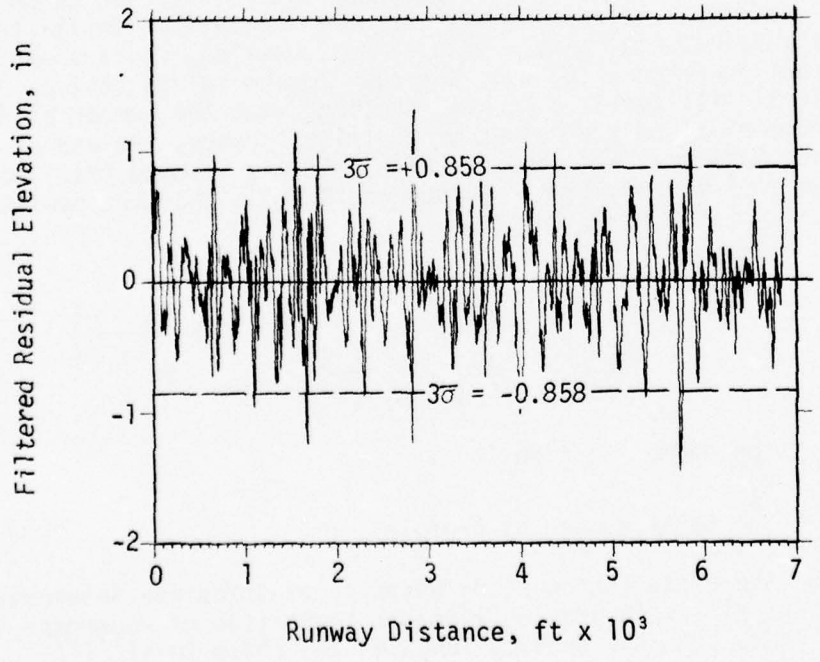

(b) Filtered Profile

Figure 10. Demonstration of Exceeded Reference Levels

are independent, they can also be treated as random variables forming their own density function, and their own first and second moments are significant overall property statistics. An example of a detailed roughness statistic is the $3\bar{\sigma}$ = 0.837 in. level. Any single bump which exceeds this level must be considered abnormal to some extent. It is possible, for instance, to have a profile with a lower σ level than the average that contains several very bad bumps which exceed the $3\bar{\sigma}$ level. Therefore, it may be necessary to repair such rough spots, even though the overall profile is relatively smooth. Consequently, it is desirable to study the distribution of the peak values of all profiles collectively in order to classify specific abnormal rough spots.

At this time 21 independent profiles (table 3) are available from which statistical information can be estimated. Since the overall roughness properties can be judged directly from the profile σ values given in table 3, it is desirable to know the distribution properties of these values. With the small number of entries, the resulting density function would be crude and a poor approximation of the true density function obtainable if many profiles were available. However, with the simplifying assumption that the filtered profile distributions are normal, an analytical approach to estimating this density function can be applied.

Since all of the relative kurtosis values, β_2, in table 3 are greater than 3, the distributions are not normal. Nevertheless, it is still expected that this simplifying assumption will not cause serious effects and that the results will be more realistic than the crude results obtained otherwise. With this assumption, it is shown in the literature (reference 10) that the mean square values (the μ_2 values in table 3) will follow a χ^2-distribution, with the number of degrees-of-freedom equal to the number of profiles. Hence, instead of using the crude empirical distribution of μ_2, it was assumed that these values followed a χ^2-distribution. Reference 10 shows that the density function for μ_2 can then be written

$$f(\mu_2) = \frac{1}{\Gamma\left(\frac{K-1}{2}\right)} \left(\frac{K}{2\bar{\sigma}^2}\right)^{\frac{K-1}{2}} \mu_2^{\frac{K-3}{2}} e^{-\left(\frac{K\mu_2}{2\bar{\sigma}^2}\right)} \qquad (11)$$

where Γ = the gamma function
$\bar{\sigma} = \sqrt{\bar{\mu}_2}$
K = the total number of profiles.

It is not the distribution of μ_2 which is of immediate interest, since the rms (or σ) levels provide a direct indication of roughness. Reference 10 shows that the density function for the σ level, $f'(\sigma)$, can be derived from eq. (11):

$$f'(\sigma) = f(\mu_2)\left|\frac{d\mu_2}{d\sigma}\right| \tag{12}$$

where $\mu_2 = \sigma^2$, or $d\mu_2/d\sigma = 2\sigma$. Then

$$f'(\sigma) = \frac{2}{\Gamma\left(\frac{K-1}{2}\right)}\left(\frac{K}{2\bar{\sigma}^2}\right)^{\frac{K-1}{2}} \sigma^{K-2}\, e^{-\left(\frac{K\sigma^2}{2\bar{\sigma}^2}\right)} \tag{13}$$

In eq. (11), the χ^2 variable was $K\mu_2/\bar{\mu}_2$; a distribution of χ^2 has a mean value of K and a variance of 2K. The mean of K corresponds to $\mu_2 = \bar{\mu}_2$; thus, $\bar{\sigma} = \sqrt{\bar{\mu}_2}$. The variance of 2K implies that the standard deviation of χ^2 is $\sqrt{2K}$. It is desirable to find the percentile levels above $\bar{\mu}_2$ (and $\bar{\sigma}$) which correspond to one, two, and three standard deviations, for the 21 profiles (i.e., K = 21), the respective values of σ (denoted with primes) were calculated as follows:

$$\bar{\sigma} = \sqrt{\bar{\mu}_2} = 0.27882 \text{ in.}$$

$$\sigma' = \bar{\sigma}\left(1 + \frac{\sqrt{2K}}{K}\right)^{1/2} = 0.31895 \text{ in.}$$

$$\sigma'' = \bar{\sigma}\left(1 + \frac{2\sqrt{2K}}{K}\right)^{1/2} = 0.35457 \text{ in.}$$

$$\sigma''' = \bar{\sigma}\left(1 + \frac{3\sqrt{2K}}{K}\right)^{1/2} = 0.38692 \text{ in.} \tag{14}$$

The density function for the filtered profile rms levels, given by eq. (13), is plotted in figure 11 with the levels of eq. (14) shown for reference. Profile rms levels falling to the left of σ' may be considered average, indicating no repair is needed; those falling between σ' and σ'' must be considered marginal, possibly indicating the need for overall smoothing; those falling above σ'' should be considered extreme, indicating immediate overall smoothing is required. It is interesting to note that DCA 18, which has been the subject of many complaints has an rms level above σ''. Also, without knowledge of this statistical work, an effort was begun to repair BGTL 16, the rms level of which falls above σ'''.

It cannot be too strongly emphasized that the rms density function shown in Figure 11 classifies profiles in an overall manner, based on the 21 available profiles. Such a presentation does not show abnormal

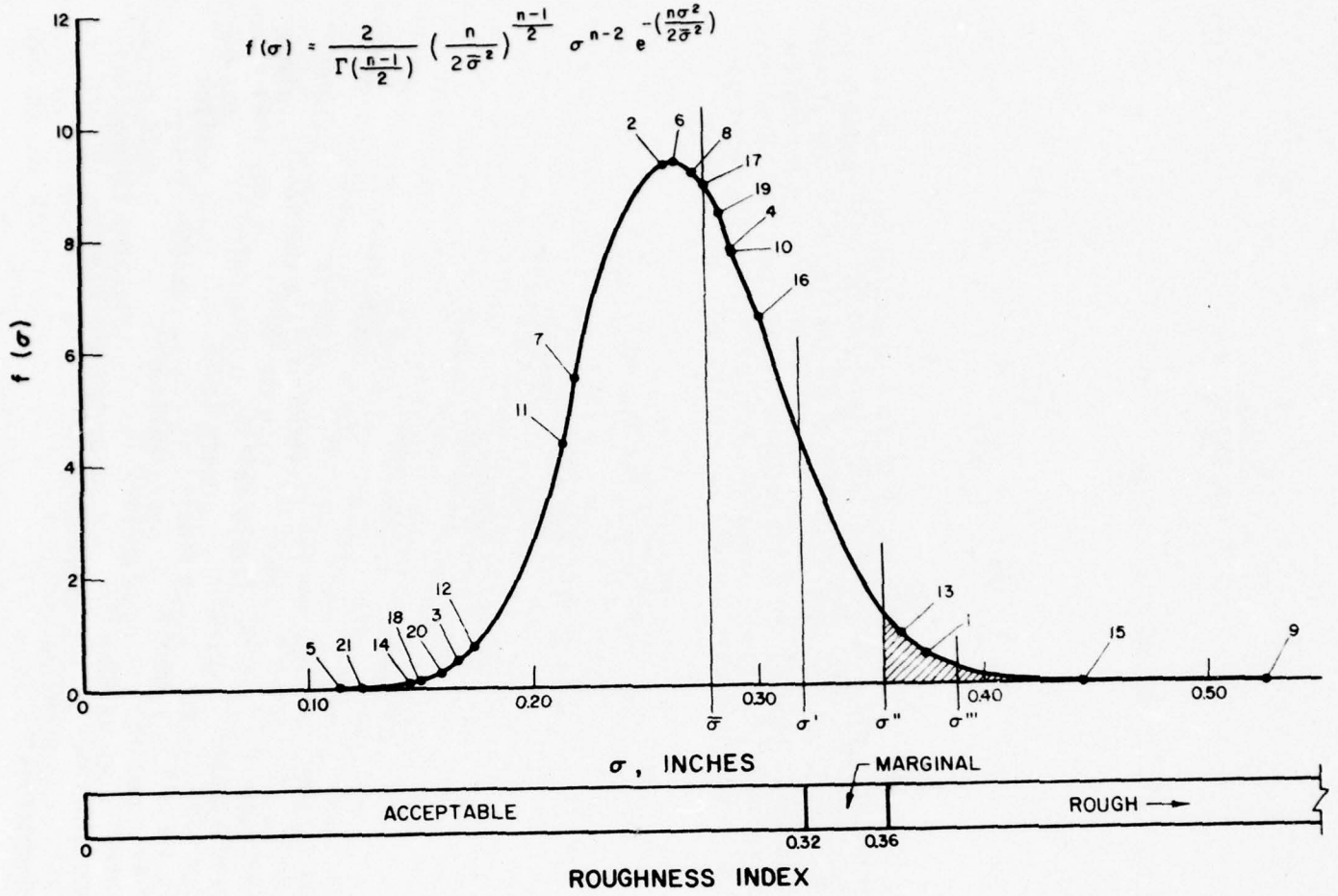

Figure 11. Probability Density Function of Profile RMS (σ) Levels

rough spots, which can exist even on the smoothest runways. For this reason, it is important to analyze peaks statistically. An example of this condition is shown by OKC TE in table 3. Note that this profile is relatively smooth (point 7, figure 11). However, this profile has one very rough spot which might be found highly abnormal. Such a subjective rating can only be quantified by a rigorous analysis of peaks such as that described in reference 11. It is therefore strongly recommended that this work be continued in the future.

Spectral Densities

It is usually desirable to transform time or space history random data into the frequency domain for the purpose of identifying dominant frequencies or wavelengths. Reference 6 states that the primary purpose of spectral analysis is to identify periodic data. For profile data, most primary statistical information can be obtained from the moments as previously discussed; the only reason for undertaking spectral analysis was to detect periodic waves which might excite the dominant fundamental modes of vibration of an aircraft. The profile forcing function frequency, if a periodic wave does exist, will be directly proportional to the aircraft velocity.

Obtaining the spectral densities of the available profiles for the sole purpose of detecting periodic waves was relatively simple. Previous attempts to use profile spectral analysis can be found in reference 12 and other documents, some of which are listed in that reference. In these studies, displacement spectral density was used as a function of wavelength. An attempt was made here to modify the displacement and wavelength variables to render the spectral densities more revealing in terms of aircraft response.

The fundamental frequencies of an aircraft are given in hertz, and they vary between about 0.5 and 4.0 Hz for the first three modes. The profile appears as a time-varying forcing function to an aircraft, and the time scaling changes as the velocity changes. It is therefore convenient to form modified spectrum plots so that excitation frequency (rather than wavelength) can be detected quickly if the taxi velocity is known. Figure 12 shows such a modified displacement spectrum of the filtered profile given in figure 10. Use of this spectrum is demonstrated as follows. Assume that it is desired to know if the small spike at point A (figure 12) is evidence of a dangerous periodic wave, given the significant fundamental aircraft frequency, F, of 1.0 Hz. The modified frequency, FKO, on the horizontal scale is about 0.035 Hz/knot. The required aircraft taxi velocity, V, is given in knots and is quickly calculated as

$$V \approx \frac{F}{FKO} = \frac{1.0}{0.035} = 28.5 \text{ knots}$$

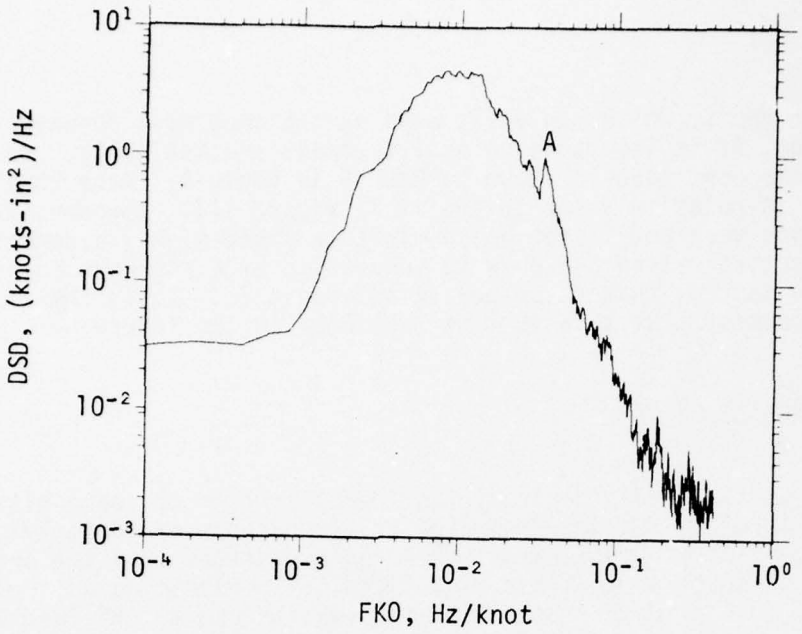

(a) Modified Displacement Spectrum

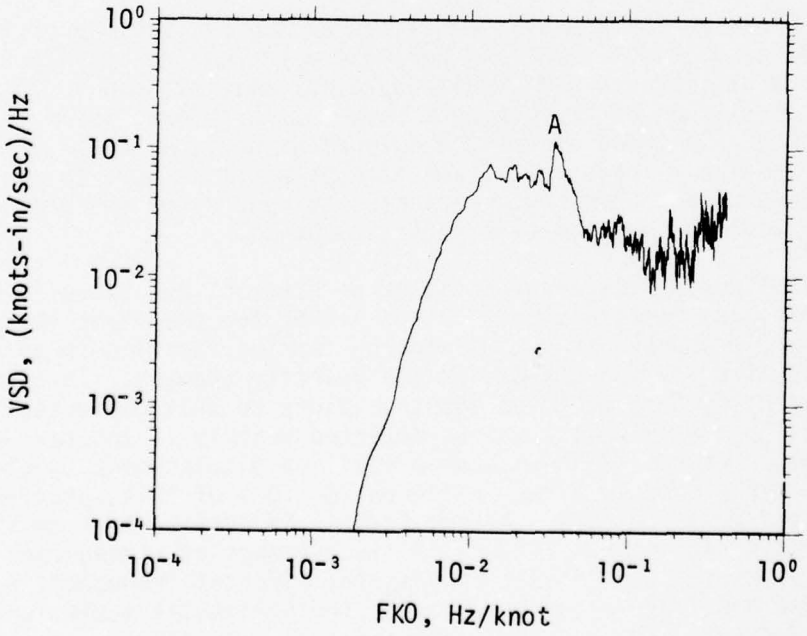

(b) Modified Velocity Spectrum

Figure 12. Modified Displacement and Velocity Spectra

A large aircraft response will probably not occur at such a low taxi velocity; therefore, it must be concluded that the spike at point A does not depict a significant periodic wave in the profile. From another point of view, consider an aircraft with a dominant frequency, F, of 0.8 Hz taxiing at 80.0 knots. For this frequency to be excited, the modified spectrum must then show a spike at

$$FKO = \frac{F}{V} = \frac{0.8}{80} = 0.01 \text{ Hz/knot}$$

Studying only the displacement spectrum of a profile is not sufficient. This is demonstrated by again using the simple oscillator shown in figure 1. Now the mass is analogous to the body of the aircraft and the spring and dashpot represent the landing gear. The forcing function, f(t), is applied to the base of the oscillator instead of to the mass and can be expressed as

$$f(t) = 2\eta\omega_o\dot{u}(t) + \omega_o^2 u(t) \qquad (15)$$

where $u(t)$ = the profile displacement as a function of time
$\dot{u}(t)$ = the time derivative of $u(t)$, or the vertical velocity.

Hence, the forcing function is composed of both the displacement and the velocity time histories. If the spectral densities of $\dot{u}(t)$ and $u(t)$ are denoted as functions of frequency, $V(\omega)$ and $U(\omega)$, reference 10 shows that if the displacement spectrum is known, the velocity spectrum can be calculated directly; i.e.,

$$V(\omega) = \omega^2 U(\omega) \qquad (16)$$

where ω = the frequency.

Hence, what may appear to be a harmless spike at a certain frequency in the displacement spectrum may have an amplified effect in the velocity spectrum. The velocity spectrum obtained from the displacement spectrum in figure 12a is shown in figure 12b. The spike at point A is more pronounced than the corresponding spike in figure 12a, thus demonstrating the effect. The significance of such spikes can be evaluated in a quantitative manner. The rms displacement or velocity at the frequency of the spike is found by taking the square root of the area between the half-power points--a procedure defined in detail in references 1, 6, and 7. Expected peak values of displacement and velocity can then be obtained by taking three times the rms values, or by the more preferred method of extremal analysis. Finally, the peak values can be compared to strut design and failure criteria for significance. Such an evaluation was beyond the scope of time and funding for this example.

In summary, there are no statistics available from the profile spectral densities which cannot be found more easily in the time or space domains. The sole purpose for monitoring this information was to detect dangerous periodic waves, which are not likely to be found on existing operational runways.

AIRCRAFT RESPONSE DATA

Aircraft response is a function of aircraft configuration and structural dynamics properties, runway profile, and taxi velocity. Response data should be considered secondary in importance to profile data. Many additional variables are involved, most of which are non-causal. Thus, response data should be analyzed only in support of conclusions derived from analyzing profile data. It is recalled that avionic maintenance, structural fatigue, and human vibration tolerance are all functions of aircraft response. Some useful aspects of response data are discussed below.

The aircraft velocity, or forward momentum, is the primary source of energy from which structural response can be excited. Although other less significant sources of energy may exist, the kinetic energy from forward motion is $1/2(mV^2)$, where m is the aircraft mass and V is the velocity. Hence, it may be expected that structural vibration response is related to horizontal velocity. On the other hand, if this velocity is such that lift is significant, the structural vibration is subdued even though the velocity is high and the landing gear is still in contact with the runway. Therefore, it is expected that an aircraft has a range of taxi velocities in which the vibration is a maximum for all possible configurations. In effect, these comments imply that aircraft response properties must be categorized according to the following:

(1) type of aircraft,

(2) aircraft configuration,

(3) taxi velocity, and

(4) runway profile.

The total problem appears formidable at present, but there are several techniques which can be helpful immediately.

The random runway profile data contain broad band noise, with negligible periodic information. In contrast, the aircraft response data are still random, but are composed of narrow-band random data generated by the aircraft's modes of vibration at relatively discrete frequencies. These response data are highly periodic, for the most part, reflecting

the fundamental frequencies of structural vibration. Therefore, spectral analysis of the response data is considerably more meaningful than that discussed in relation to profile data.

The amplitude and frequency content of response data are of primary concern. So far, accelerometers have been used to monitor response data, and the data time histories are calibrated in units of g. Amplitude information is most easily extracted directly from the acceleration time history, while frequency content can be observed from a frequency domain transformation of the data. Because of the superposition of the response from one bump on that from another, it is nearly impossible to identify the specific bump which caused a response g-level to exceed a certain limit, except in cases where single, well-defined bumps were obvious from the profile. In general, it is impractical to locate rough spots in a profile by studying the response data.

The acceleration time history at the pilot station for a Boeing 727-100 taxiing at 65 knots on DCA 18 is shown in figure 13a. Aircraft weight in this case was about 129,500 lb. The corresponding response for the same type of aircraft (142,000 lb in this case) taxiing at 60 knots on OKC 30 is shown in figure 13b. These two runs were selected for comparison because they were the most similar runs for different profiles from all the experimental response data collected. In the first case, the taxi velocity was 12 percent faster, and in the second case the gross weight was 10 percent heavier; to some extent, these differences are compensating.

It was desirable to obtain the spectral densities over 40-second time intervals, even though the traces in figure 13 were not as stationary as preferred. The poor stationary properties imply that some error in amplitude will exist in the spectral density presentations, although the primary frequency information should be sufficiently accurate for this discussion. The respective acceleration spectral densities are shown in figure 14. The frequencies for the fundamental rigid-body modes (pitch and plunge) are marked on these plots. In each case, the first mode occurred at about 1.0 Hz, and the second at about 1.5 Hz. If the two experiments had been closely controlled (which they were not), this information would be much more meaningful and conclusive. However, the significant point is that a linear mechanical system responds dominantly at its fundamental modes from random excitation (reference 1). Hence, if only the profiles differed in these two experiments, the variations in corresponding frequencies would be caused by the difference in the overall profile properties, and this would be an indicator of the significance of strut nonlinearities; therefore, this information is extremely useful in checking the theoretical results from the TAXI code. Even though the profiles are different, the fundamental mode frequencies are clearly defined and are within a reasonable percentage of each other. In checking the TAXI code results with such experimental data, it is important that the fundamental frequencies and overall rms acceleration amplitudes from

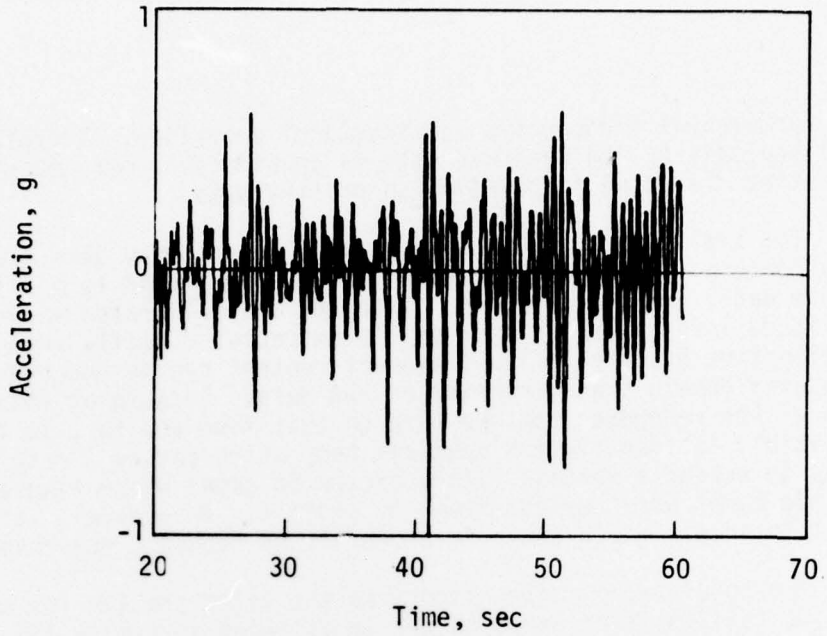

(a) Boeing 727-100 at 65 Knots on DCA 18

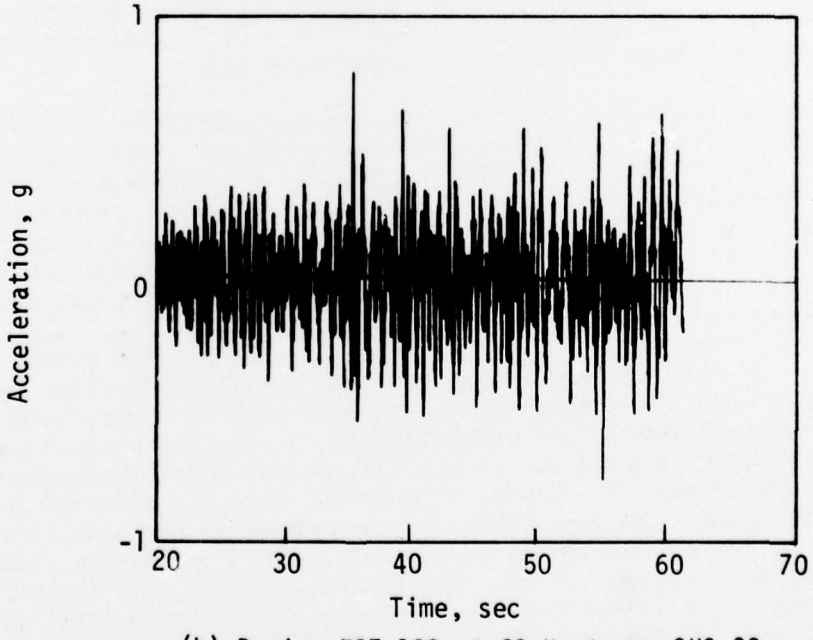

(b) Boeing 727-100 at 60 Knots on OKC 30

Figure 13. Pilot Acceleration from Different Profiles

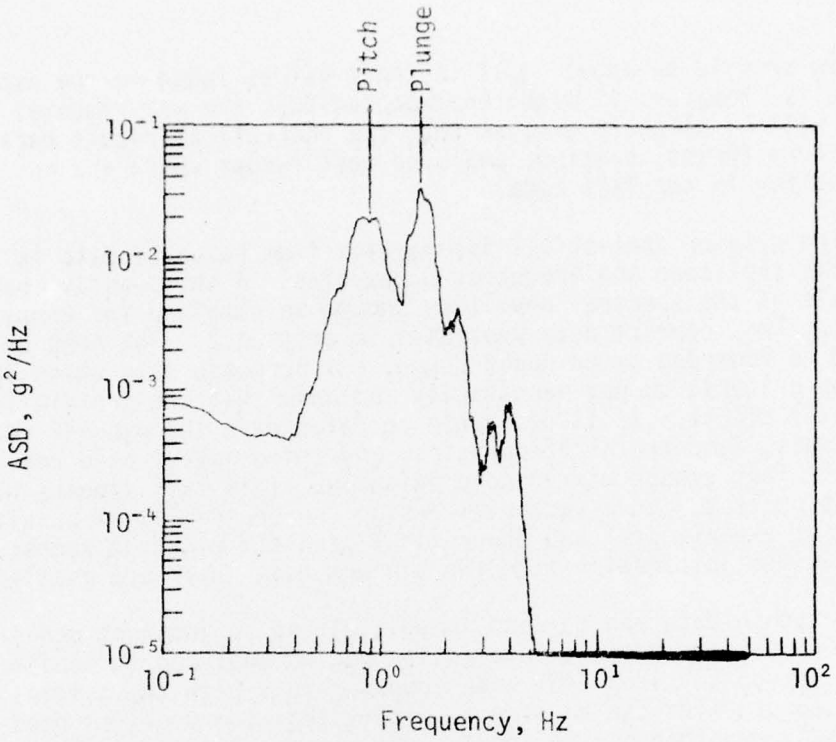

(a) Boeing 727-100 at 65 Knots on DCA 18

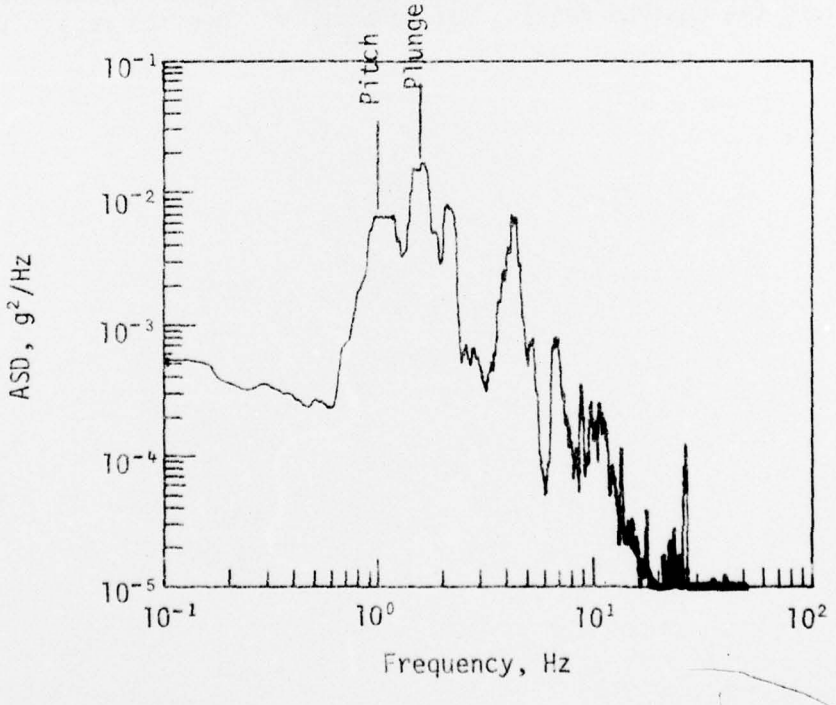

(b) Boeing 727-100 at 60 Knots on OKC 30

Figure 14. Acceleration Spectral Densities from Different Profiles

a given profile be about equal to those values found in the experiment. Generally, however, it might be expected that the experimental rms level will be slightly greater than the theoretical result because of nonuniform thrust, braking, and wind gust forces which are not accounted for in the TAXI code.

The primary statistical information from response data is therefore rms amplitude and frequency properties. A third-octave band analysis of the spectral densities should be obtained for comparison with the AMRL comfort data presented in section 2. The AMRL criteria should be regarded as an upper bound, but response data which fall below the criteria do not necessarily indicate that the profile is sufficiently smooth. It is desirable to categorize the overall rms amplitudes, fundamental frequencies, and third-octave band rms levels into the four groups mentioned previously. This task appears cumbersome at present, and a factorial design (reference 13) of a suitable matrix of experimental and theoretical problems might be necessary to gain maximum information from the minimum data which are available.

Response data can be used immediately in an indirect manner, however. First, the profile information can be analyzed to locate specific rough spots. Then TAXI code computer runs with the original and corrected profiles can be made to verify that the profiles have been adequately smoothed in the appropriate areas. Thus, the response data and the TAXI code can be used to verify that the profile corrections will yield the desired results before money is spent to repair the runway.

SECTION 4

SUMMARY

The absorbed power technique has not been sanctioned by AMRL because of disagreement with experimental data. If this technique were valid, rough segments of a runway could be identified (without precision) from aircraft response data. Also, a single scalar quantity (e.g., 6 W) could be used as the limiting criterion. However, no rationale exists for establishing a suitable averaging time, and changes in averaging time yield proportional changes in absorbed power. If the AMRL data are recognized as more accurate, then the vibration response of a human must be significantly different from that of a system of damped oscillators of the type shown in figure 1; the power absorbed by the human damping mechanism may not be the only source of discomfort.

The third-octave band technique recommended by AMRL is strictly empirical and needs no theoretical model for its implementation. This method is only slightly more complicated than the absorbed power approach; a rms g-level in each frequency band is needed as a criterion. The problems encountered do not reflect the inadequacy of the technique itself. For example, the available response data were usually well below the comfort criteria levels in all bands. This should be sufficient proof that passenger discomfort is not the real criterion of concern. However, more studies might be made at different aircraft velocities to determine if there is a normal operating range for each aircraft in which the criteria are exceeded for a profile known to be rough, such as that for DCA 18. At present, the third-octave band comfort criteria can be recognized as an upper bound. In the case where the criteria were exceeded (on BGTL 16), repairs were considered mandatory before the results of this study had reached the involved personnel. A major problem in applying this technique is that criteria were not available for exposure times of less than 1 minute.

The lack of more appropriate human failure criteria and the assumption that component and structural failure are not of paramount interest led to the statistical classification of the available data. Such a classification arranges all statistical parameters on a relative, but accurate, scaling basis. For example, the rms values in table 3 can be arranged in increasing order, and the degree of roughness sensed by passengers should be in direct (but possibly nonlinear) proportion to these rms values. The same statement should apply for the rms values of slopes and slope changes. The mean square values in table 3 follow a χ^2 distribution which has a mean, median, and standard deviation of statistical significance. As the number of available profiles is increased, this distribution should approach a normal distribution. From the distribution of mean square values, the

distribution of rms values can be derived; this provides a direct indicator of overall roughness properties. Another highly useful statistical study would be the determination of the distribution of peak values of the profiles. Parameters from this study should be used as indicators for detailed rough spots. The technique for such an analysis is given in reference 11.

Aircraft response data should also be analyzed statistically. The major problem in this effort would be to design a matrix of problems which would yield maximum information with minimum computer runs or experimental data. Because of the variables, i.e., aircraft type and configuration, taxi velocity, and runway profile, the amount of data required before a meaningful classification can be made is expected to be quite large. Response data are periodic; hence, the spectral analysis (a statistical technique) of response data reveals the vibration modes of the aircraft. The modal frequencies for a particular aircraft should be consistent and almost independent of the runway profile; this information is valuable in comparing theoretical results and experimental response data as they become available. In summary, the analysis of response data in the time, amplitude, and frequency domain has been performed infrequently in the past, and an organized approach to this problem in the future is highly desirable. For the immediate future, theoretical response data can be used to verify hypothetical profile correction effectiveness.

SECTION 5

CONCLUSIONS AND RECOMMENDATIONS

CONCLUSIONS

The use of statistical methods has been shown to be a logical and viable method for quantifying runway roughness. This approach eliminates the necessity of modeling the aircraft and extending conclusions from the dynamic response properties to form subjective ratings of ride quality. In general, techniques which involve aircraft response, including both human and structural response methods, cannot be relied upon to yield precise locations of abnormal rough spots. The direct approach of analyzing profile roughness is superior in this respect.

The empirical human response data from AMRL are more generally accepted on an international basis than data generated from the absorbed power method. However, neither of these techniques is applicable for the phenomenon of concern, since the published human comfort levels are well above those experienced by humans in taxiing aircraft. The use of alternate criteria suggested by AMRL cannot be recommended until complete documentation is available.

RECOMMENDATIONS

The use of statistical methods to establish roughness criteria, as demonstrated partially in this report, is recommended. The criteria shown in figure 15 are recommended as quantitative definitions of overall pavement roughness. A corresponding scale should be furnished for detailed roughness when the information becomes available.

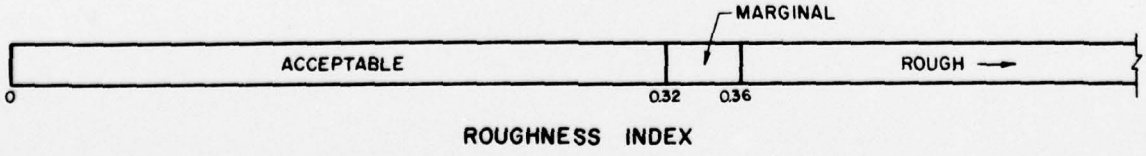

Figure 15. Recommended Quantitative Definitions of Overall Pavement Roughness

Continuation of this effort to use extremal statistics to assess detailed roughness is strongly recommended. The use of response methods is still recommended, but for verification purposes rather than for primary assessment of roughness. The collection of response data for future efforts should be more closely controlled and organized so that a maximum amount of information can be extracted from a minimum number of experiments.

REFERENCES

1. Harris, C. M., and Crede, C. E., *Shock and Vibration Handbook* (three volumes), McGraw-Hill Book Company, Inc., New York, 1961.

2. Lins, W. F., *Human Vibration Response Measurement,* Technical Report No. 11551, U.S. Army Tank-Automotive Command, Warren, Michigan, 1972.

3. Pradko, F., Lee, R. A., and Kaluza, V., *Theory of Human Vibration Response,* ASME publication 66-WA/BHF-15, The American Society of Mechanical Engineers, United Engineering Center, New York, New York, August 1966.

4. Lee, R. A., and Pradko, F., "Analytical Analysis of Human Vibration," *SAE Transactions,* Vol. 77, Paper 680091, 1968.

5. *Guide for the Evaluation of Human Exposure to Whole Body Vibration,* Draft International Standard ISO/DIS 2631, UDC534.1:612.014.4, submitted for approval to the ISO Central Secretariat 28 April 1972.

6. Bendat, J. S., and Piersol, A. G., *Random Data: Analysis and Measurement Procedures,* Wiley-Interscience, John Wiley & Sons, Inc., New York, 1971.

7. Crandall, S. H., and Mark, W. D., *Random Vibration in Mechanical Systems,* Academic Press, New York, 1963.

8. Hahn, G. J., and Shapiro, S. S., *Statistical Models in Engineering,* John Wiley & Sons, Inc., New York, 1967.

9. Gold, B., and Rader, C. M., *Digital Processing of Signals,* McGraw-Hill Book Company, Inc., New York, 1969.

10. Ostle, B., *Statistics in Research,* The Iowa State University Press, Ames, Iowa, 1963.

11. Gumbel, E. J., *Statistics of Extremes,* Columbia University Press, New York, 1958.

12. Morris, G. J., *Response of a Turbojet and a Piston-Engine Transport Airplane to Runway Roughness,* NASA TN-D-3161, Langley Research Center, Langley Station, Hampton, Virginia, December 1965.

13. Mendenhall, W., *The Design and Analysis of Experiments,* Duxburg Press, Wadsworth Publishing Co., Inc., Belmont, California, 1968.

APPENDIX

FILTERING WITHOUT PHASE SHIFT

Digital filtering is presented in detail in references 6 and 9. In this work it was considered important to prevent phase shifting of the data points, as is usually the case when a nonlinear phase filter is used. Most available digital filters have a nonlinear phase property. The effect is that a peak from a filtered profile is shifted slightly from its true position and not all peaks are shifted by precisely the same amount. To avoid this undesirable effect, either a linear (or zero) phase filter can be used, or a more commonly available nonlinear phase filter can be used twice, filtering the data once in each direction.

The double-filtering technique is explained mathematically as follows. Let $f(x)$ be a raw runway profile. For convenience, the filtering is assumed to be accomplished in the frequency domain; in which case, let $F(\Omega)$ be the Fourier transform of $f(x)$. The filter may also be represented in the frequency domain by the complex function $H(\Omega)$. The fact that $H(\Omega)$ is generally complex implies that it has magnitude and phase parts, and the phase part is generally nonlinear. The first filtering operation is performed on the raw profile from left to right; thus

$$\vec{F}(\Omega) = F(\Omega) * H(\Omega) \tag{A-1}$$

where $\vec{F}(\Omega)$=the Fourier transform of the filtered runway profile, and the asterisk denotes complex multiplication. The second filtering, $H(-\Omega)$, is performed from right to left; thus

$$\begin{aligned} \overleftarrow{\vec{F}}(\Omega) &= \vec{F}(\Omega) * H(-\Omega) \\ &= F(\Omega) * H(\Omega) * H(-\Omega) \end{aligned} \tag{A-2}$$

Here, $\overleftarrow{\vec{F}}(\Omega)$ is the Fourier transform of the double-filtered profile. Eq. (A-2) may now be written

$$\overleftarrow{\vec{F}}(\Omega) = F(\Omega) * |H(\Omega)|^2 \tag{A-3}$$

In this manner the phase property of the filter has been eliminated. If the modulus of the filter, $|H(\Omega)|$, is unity in the frequency passband of interest, there will be a small amplitude reduction at the cutoff frequency; this may be ignored. The final filtered runway profile

is then obtained by taking the inverse Fourier transform of $\overleftarrow{F}(\Omega)$.

If a digital recursive filter is used, it is necessary to allow an extended number of horizontal (or zero) points on each side of the raw profile before the filtering operation is performed. This is necessary because such a filter manipulates a fixed number of data points at a time. When the ends of the profile are approached, the filtering must be allowed to extend to a smooth section, or an undesirable *glitch* will appear at each end.

ABBREVIATIONS, ACRONYMS, AND SYMBOLS

A_i	Peak g-level of i^{th} frequency
AMRL	Aerospace Medical Research Laboratory
A_{rms}	rms g-level
ATC	Army Tank-Automotive Command
F	Frequency
FKO	Modified spectrum ordinate
GKO	Modified spectrum abscissa
K	Total number of profiles
K_i	Transfer function constant at i^{th} frequency
N	Total number of discrete frequencies; total number of points
P	Absorbed power
P(z)	Probability distribution function
T	Time over which power is averaged
U	Profile displacement spectral density
V	Profile velocity spectral density; aircraft taxi velocity
f(t)	Time-varying forcing function applied to mass
$f'(\sigma)$	Probability density function for σ levels
i	Frequency index
k	Spring constant
m	Mass
n_i	Number of data points in i^{th} increment
p(z)	Probability density function
rms	Root-mean-square

ABBREVIATIONS, ACRONYMS, AND SYMBOLS (Continued)

u	Profile displacement
$\dot{u}$	Profile vertical velocity
$v(t)$	Vibration velocity
x	Displacement of mass; distance along runway
$\dot{x}$	Velocity of mass
$\ddot{x}$	Acceleration of mass
z	Displacement amplitude
Γ	Gamma function
$\sqrt{\beta_1}$	Relative skewness
β_2	Relative kurtosis
η	Damping ratio
μ_j, $j = 1, 2, 3, 4$	First four statistical moments
$\overline{\mu}_j$	Average j^{th} moment
χ^2	Chi-square probability distribution function
ω_o	Natural frequency of oscillator

GPO 912-408